



Review

Identification of Landslide Precursors for Early Warning of Hazards with Remote Sensing

Katarzyna Strzabała , Paweł Ćwiakała * and Edyta Puniach

AGH University of Krakow, Faculty of Geo-Data Science, Geodesy, and Environmental Engineering,
30-059 Cracow, Poland; strzabal@agh.edu.pl (K.S.); epuniach@agh.edu.pl (E.P.)

* Correspondence: pawelcwi@agh.edu.pl

Abstract: Landslides are a widely recognized phenomenon, causing huge economic and human losses worldwide. The detection of spatial and temporal landslide deformation, together with the acquisition of precursor information, is crucial for hazard prediction and landslide risk management. Advanced landslide monitoring systems based on remote sensing techniques (RSTs) play a crucial role in risk management and provide important support for early warning systems (EWSs) at local and regional scales. The purpose of this article is to present a review of the current state of knowledge in the development of RSTs used for identifying landslide precursors, as well as detecting, monitoring, and predicting landslides. Almost 200 articles from 2010 to 2024 were analyzed, in which the authors utilized RSTs to detect potential precursors for early warning of hazards. The applications, challenges, and trends of RSTs, largely dependent on the type of landslide, deformation pattern, hazards posed by the landslide, and the size of the area of interest, were also discussed. Although the article indicates some limitations of the RSTs used so far, integrating different techniques and technological developments offers the opportunity to create reliable EWSs and improve existing ones.

Keywords: landslides; early warning; detection; monitoring; prediction; precursor; hazard assessment



Citation: Strzabała, K.; Ćwiakała, P.; Puniach, E. Identification of Landslide Precursors for Early Warning of Hazards with Remote Sensing. *Remote Sens.* **2024**, *16*, 2781. <https://doi.org/10.3390/rs16152781>

Academic Editors: Thomas Oommen and Mirko Francioni

Received: 20 June 2024

Revised: 17 July 2024

Accepted: 22 July 2024

Published: 30 July 2024



Copyright: © 2024 by the authors. Licensee MDPI, Basel, Switzerland. This article is an open access article distributed under the terms and conditions of the Creative Commons Attribution (CC BY) license (<https://creativecommons.org/licenses/by/4.0/>).

1. Introduction

Landslides significantly affect the quality of life in the local community and the safety of buildings. Their occurrence is complex and depends on many natural and anthropogenic factors. The most significant natural factors leading to the formation of mass movements, such as landslides, include geological and geomorphological conditions, heavy and prolonged rainfall, topography, groundwater, freeze–thaw, and wetting–drying cycles [1]. Identifying and monitoring these factors and understanding their impact on landslides is key to effective risk management [2] and minimizing the effect of landslides by, among other things, taking warning and evacuation measures [3].

An essential step in controlling the risks associated with mass movements is the introduction of continuous monitoring [4] and EWS [5]. The purpose of monitoring is the systematic and continuous processing of acquired observations about the changes occurring in areas prone to landslides. On the other hand, analyzing data obtained from real-time monitoring or historical data, which forms the basis of early warning systems, allows potential risks to be identified. Landslide monitoring and EWS have mainly relied on in situ measurements [6]. Various techniques were used for this purpose, such as geodetic, geotechnical, geophysical, and hydrological measurements, utilizing inclinometers, piezometers, total stations, and GNSS receivers, among others [7]. However, RSTs, including Synthetic Aperture Radar (SAR), Ground-Based Interferometric Synthetic Aperture Radar (GB-InSAR), multispectral and optical images from unmanned aerial vehicles (UAV) and optical satellites, Light Detection and Ranging (LiDAR), which include TLS (Terrestrial Laser Scanning) and ALS (Airborne Laser Scanning), Infrared Thermography (IRT), are

becoming increasingly popular. These techniques enable earth observation from satellite, airborne, and ground altitudes [8–10], contrary to traditional techniques, and can be implemented on a regional scale. The developments in landslide hazard monitoring also allow the detection of various landslide precursors. These are defined as features or phenomena showing displacements over time or abnormal changes in monitored features, which can significantly increase the landslide probability. Their identification aims to minimize the risk of landslides by detecting potential hazards in advance and taking appropriate responses [3]. The main precursors include groundwater levels, soil moisture, movements and deformations of the land surface, thermal anomalies, and topographic changes. Based on these data, detailed analyses are often carried out to map landslide distributions for public safety and emergency management [11]. Integrating data from various sources, such as geodetic measurements, radar systems, satellite images, and meteorological data, allows for a comprehensive approach to landslide hazard analysis. By analyzing these data and detecting characteristic changes in the analyzed factors over time for landslide areas identified in the past, the potential risk of hazards in potential new areas can be assessed more effectively [12]. All this creates the opportunity to predict landslides even several days before their occurrence [13,14].

This paper reviews articles and discusses the potential and use of RSTs to identify landslides for early warning of hazards between 2010 and 2024. This review focuses on identifying recent advances and research trends in identifying landslide precursors based on an in-depth analysis of nearly 200 scientific articles. The data collection process was conducted using the PRISMA schema, providing a transparent approach to literature selection. This review included a variety of RSTs, such as SAR, GB-InSAR, optical multispectral and hyperspectral imaging, LiDAR, and IRT. These techniques were evaluated for their effectiveness in identifying landslide precursors, as well as their advantages and limitations.

2. Data Collection

In this literature review, the Scopus database was used to collect all possible scientific inputs in which authors use RSTs to detect potential precursors for early warning of hazards. The diversity of publication types in the Scopus database, i.e., scientific journals, conference papers, books, technical reports, and other materials published in English, allows for a more comprehensive literature review than in the Web of Science (WoS). On the other hand, Google Scholar (GS), which has less precise and advanced tools for filtering results, may be less effective in providing articles that comply with established criteria [15]. Scopus and WoS data in all areas are considered a subset of the GS database [16]. However, GS contains a lot of duplicate citations [17], which can significantly affect the quality of the literature review. In addition, Scopus is highly correlated with the GS article database in life and earth sciences (93%), indicating a high level of coverage and compatibility between these databases [16]. According to the research, almost 99.11% of the journals indexed in WoS are also included in the GS database [18]. Scopus also has an advantage over other databases by offering advanced tools for analyzing scientific data, allowing detailed filtering of data, trend research, and analysis of results.

The data collection for the literature review was conducted in several stages. The first was to define the time range of the review (2010–2024) and to select articles written in English. Four main criteria were then determined and used to search the Scopus database. These included the following keywords: (1) landslide and precursor; (2) landslide and early warning and detection; (3) landslide and early warning and monitoring; and (4) landslide and early warning and prediction. Their selection was significant in identifying critical articles that contained valuable information directly relevant to the topic under review. The first criterion defined was chosen as the primary criterion. Since the word ‘landslide’ plays a crucial role in both ‘detection,’ ‘monitoring,’ and ‘prediction’ of landslides, it was included when analyzing results from the Scopus database in the subsequent criteria. After a detailed review of many articles, the additional keyword ‘early warning’ helped narrow the selection and focus on publications presenting novel research approaches or

results that could be developed and implemented in modern EWSs. A total of 1808 search records and an additional 22 through manual and origin of the search were identified in the database (total $n = 1830$). After removing 327 duplicates, screening by title and abstract removed 1299 records. During the review of titles and abstracts, articles were rejected for three reasons:

- Reason 1: The articles were not directly related to the literature review topic. They covered various issues, including strategies for implementing EWSs, testing measurement equipment to improve the quality of data acquired, managing and transmitting measurement data, and countering various natural disasters and phenomena;
- Reason 2: The articles were not related to landslide detection, monitoring, and prediction as defined in the article [2]. Therefore, publications in which the prediction approach was based entirely on statistical or physical models and did not involve analysis of historical data, field observations, or monitoring results were excluded from the review;
- Reason 3: The articles presented the results of studies where RST was not used.

The full texts of the remaining 204 records were reviewed. On reading the full texts, 39 articles only met some eligibility criteria. The first reason was the need for more crucial information on using RST to study precursors, even though the abstract mentioned this. The second reason was the exclusion of items that were books containing a series of articles that were previously analyzed separately and included in the review. In this way, the final number of 165 articles analyzed in the remainder of the study was selected. Figure 1 shows a flow chart of the PRISMA study describing the selection process and reasons for exclusion [19].

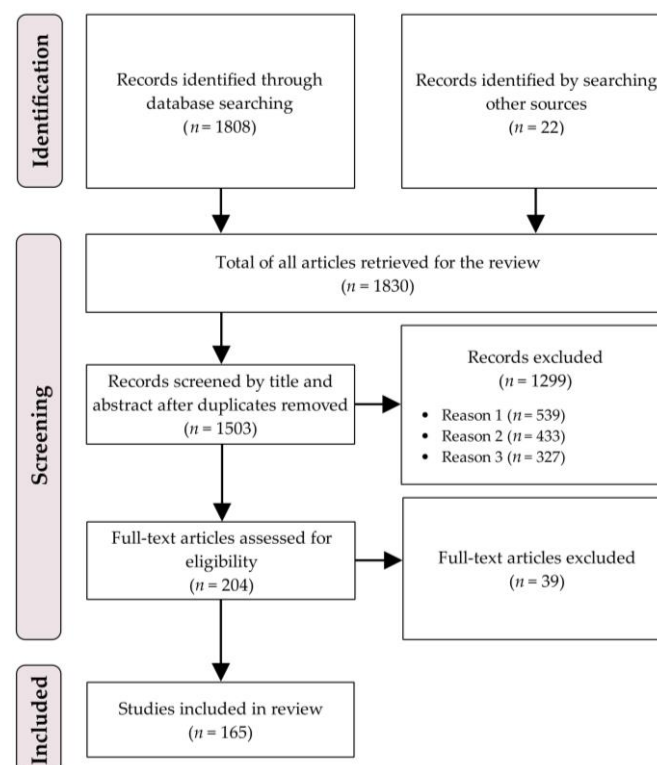


Figure 1. PRISMA flow diagram of the search process.

3. RSTs: Description and Temporal Evolution of Scientific Production

RSTs show high efficiency in investigating surface changes, allowing a systematic, time-efficient, and cost-effective view of the ground surface on a large scale. These technologies, which include SAR, GB-InSAR, optical and multispectral image acquisition, LiDAR, and

IRT, play a crucial role in EWSs, enabling the identification of ground displacements and structural changes induced by the occurrence of landslides.

This section describes the characteristics of RSTs, their sensors, and the basic processing principles used in monitoring changes in landslide areas. RSTs using optical and multispectral imaging are described separately due to their different applications and the type of analysis performed. Table 1 shows the main characteristics of the spatial data acquired using RST, i.e., the types of sensors acquiring the data, the platforms on which they are mounted, the spatial resolution, and the standard scene sizes. For satellite data, example sizes of standard maps obtained in imaging mode are given, while standard areas of studies obtained during measurements are given for the other techniques.

Table 1. Comparison of example characteristics of spatial data acquired with RSTs used to observe earth surface displacements.

RST	Sensor	Example	Spatial Resolution	Standard Scene Size
SAR	Satellite radar	Sentinel-1	Range: 1.5 m Azimuth: 3.6 m	80.1 × 80.1 km
		TerraSAR-X	Range: 0.24 m Azimuth: 0.6 m	4 × 3.7 km
		ALOS-2	Range: 3.0 m Azimuth: 1.0 m	25 × 25 km
GB-InSAR	Ground-based radar	FMCW	Range: 0.75 m Azimuth: 1.5 m	2 × 2 km
Optical images	Optical satellite sensor	WorldView-3	PAN band: 0.31 m	13.1 × 13.1 km
	Optical aircraft sensor	Leica RC-30	5 cm (500 AGL)	10 × 10 km
	Digital camera on UAV	Zenmuse P1	~1 cm (75 AGL)	2 × 2 km
Multispectral/ Hyperspectral images	Multispectral satellite sensor	Sentinel-2	10/20/60 * m	100 × 100 km
		PlanetScope	3 m	20 × 20 km
	Multispectral camera on UAV	MicaSense RedEdge-P	~5 cm (70 AGL)	2 × 2 km
LiDAR	Aerial laser scanner	Riegl miniVUX-3UAV	5 mm (100 AGL)	2 × 2 km
	Terrestrial laser scanner	RIEGL VZ-400i	1 mm (distance of 100 m)	800 m
IRT	Thermal camera on UAV	Zenmuse H20 Series	~2 cm (75 AGL)	2 × 2 km
	Handheld IR camera	Flir SC620	~6 cm (distance of 100 m)	80 × 60 m

The table uses the following abbreviations: PAN (Panchromatic), VNIR (Visible Near Infrared), SWIR (Shortwave Infrared), AGL (Height above ground level), and IR (Infrared camera). * 10 m spatial resolution bands: B2 (490 nm), B3 (560 nm), B4 (665 nm), B8 (842 nm); 20 m spatial resolution bands: B5 (705 nm), B6 (740 nm), B7 (783 nm), B8a (865a nm), B11 (1610 nm), B12 (2190 nm); 60 m spatial resolution bands: B1 (443 nm), B9 (940 nm), B10 (1375 nm).

3.1. SAR Overview

In recent years, the SAR technique has started to be used in studies related to natural hazards and has become a powerful remote sensing tool used to acquire data for vast areas. They provide a way to understand landslide movement's spatial and temporal patterns [20]. SAR sensors on various satellites (Figure 2) can penetrate clouds, enabling data acquisition in different atmospheric conditions, regardless of the time of day or season. This feature is crucial for continuous landslide monitoring and prediction [2].

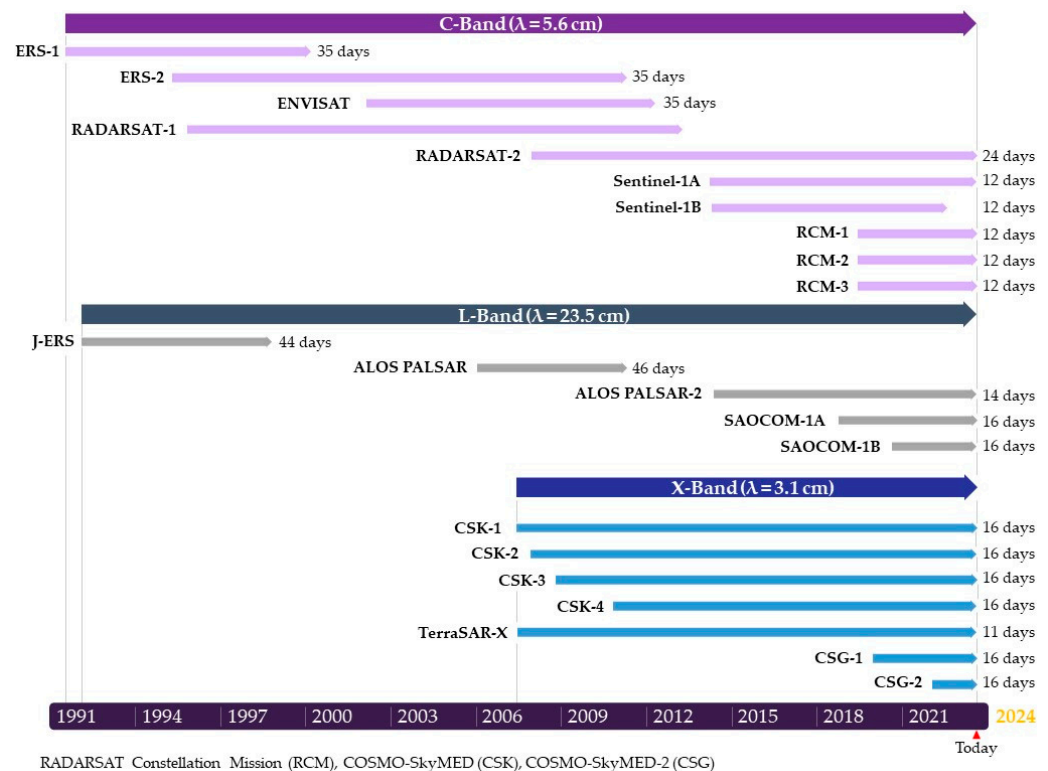


Figure 2. Selected active SAR satellites used for site monitoring; modified after [21], licensed under Creative Commons Attribution 4.0 (CC BY 4.0).

The SAR sensors can operate in different frequency bands, including the X (8–12 GHz, wavelength: 2.4–3.8 cm), C (4–8 GHz, wavelength: 3.8–7.5 cm), and L (1–2 GHz, wavelength: 15–30 cm) bands. The frequency of radar sensors determines their ability to penetrate a medium, influencing the choice of radar band based on the type of study area and research purposes [22–24]. X-band and C-band signals only penetrate the upper layers of soil and vegetation. On the other hand, L-band data are far more suitable for monitoring displacements in areas covered with dense vegetation [25] and with low correlation areas [11]. SAR images consist of pixels characterized by signal intensity, direction, amplitude, and phase values [21]. The amplitude value depends on the radar reflectance, while the phase value of a single SAR image partly depends on the distance of the sensor from the earth's surface.

Techniques such as Coherence Change Detection (CCD) [26,27], Offset Tracking (OT) [28–31], and Interferometric Synthetic Aperture Radar (InSAR) are commonly used SAR techniques for analyzing the earth's surface with high resolution and precision. The continuous development of SAR has also allowed the development of Adaptive Distributed Scatterer InSAR (ADS-InSAR) [32] and SAR Shape from Shading (SAR-SfS) [33] techniques that extend its potential and enable different approaches to data processing and analysis depending on the area under study. Among the best-known techniques for obtaining information on changes in the topography of the land surface is Differential Interferometric SAR (D-InSAR). This technique measures the difference in signal phase between successive radar image recordings over time [23,34]. However, emerging limitations related to temporal and spatial decorrelation, as well as phase interference due to the atmosphere, reduce the reliability of this technique. To overcome these limitations, In-SAR-based information can be enhanced using multi-temporal interferometric techniques (MT-InSAR) based on the analysis of large SAR image sets [35–38]. The results of MT-InSAR analyses are ground surface displacements over time. Among the most well-known and frequently used MT-InSAR techniques in landslide studies are Permanent Scatterer Interferometry (PS-InSAR) [39–43], Small BASeline Subsets Interferometry (SBAS-InSAR) [22,40,44–47],

SqueeSAR [45], Quasi PS technique (QPS-InSAR) [48], and Temporal Coherent Point InSAR (TCP-InSAR) [25,49].

Basic interferometric data analysis techniques can use different approaches, such as Single Look, Multi Look [50], and Two-Pass Interferometry [51]. The first is based on analyzing the complete information contained in a single pixel of a radar image. This allows for more detailed data, but the approach is more susceptible to noise and atmospheric interference. On the other hand, the Multi-Look technique involves grouping the pixels of the radar image. As a result of this process, the resolution of the image is reduced while improving image quality and reducing noise. The Two-Pass Interferometry approach involves accurately comparing two independent satellite overflights to determine changes in signal phase and precisely measure terrain deformation. This technique is beneficial when the displacements are dynamic and can occur between consecutive satellite visits. Backscatter is also essential for interpreting radar data [52–54]. The intensity of the scattering is used to determine land surface characteristics such as texture, soil moisture, or vegetation features.

PS-InSAR and SBAS-InSAR effectively deal with the challenges of radar signal decoherence between two consecutive satellite revisits [55]. Both techniques use many SAR images to estimate and correct atmospherically induced phase distortions. SBAS-InSAR and PS-InSAR are the main techniques for monitoring deformation using time series analysis. PS-InSAR uses highly coherently distributed points in cell resolution, while SBAS-InSAR uses spatial distribution in short baselines [40]. These techniques are primarily used in urbanized areas. Depending on the degree of vegetation cover, the SqueeSAR technique can also be used in non-urbanized areas. The technique allows ground displacement to be measured using PS points and partially coherently distributed scatterers (DS). DSs are radar targets corresponding to multiple neighboring pixels in a SAR image, characterized by similar low reflectance. They usually correspond to homogeneous areas with limited radiometric variability. These are natural scatterers, i.e., forests, agricultural fields, bare soil, wasteland, and rock surfaces. These techniques achieve high accuracy in determining land deformation, especially in the case of slow landslide movements. In contrast, the technique based on the interferogram phase may not be sufficient for rapid movements due to underestimation caused by phase unwrapping errors [56]. For comparison, the maximum detectable displacements between two interferogram acquisitions, using appropriate phase unwrapping algorithms and assuming that the data are free of noise, are 25.7, 42.6, and 46.8 cm/year for platforms such as Terra SAR-X, Sentinel-1, and ALOS-2, respectively [57]. Therefore, to determine displacements with high deformation velocities that exceed the measurement capabilities of the standard multi-interferometric approach, the OT technique is used, utilizing total amplitude information [31].

The data acquired with SAR sensors can be utilized for mapping unstable slopes [52,58], monitoring [13,59], identifying [48], characterizing landslides [21], and analyzing their evolution over time [28,60–62]. Such studies have mainly been carried out using techniques such as CCD [26], D-InSAR, MT-InSAR, and Stream Length-gradient Hotspot and Cluster Analysis (SL-HCA) [3]. However, most of them have focused on conducting detailed studies of individual landslides at the local scale [63], with significantly fewer studies conducted at the regional scale [64–66].

3.2. GB-InSAR Overview

Continuous technological advances improving the GB-InSAR quality have increased its popularity and use in various fields. The high resolution of the acquired data, the speed of acquisition, the ability to acquire data from restricted areas, and the ability to work in all weather conditions make the GB-InSAR application capable of supporting ground displacement monitoring and early warning systems [67,68]. Additionally, the ability to take measurements at much shorter intervals gives GB-InSAR a significant advantage, particularly over satellite measurements.

The operating principle of GB-InSAR is similar to that of satellite-based InSAR and enables the determination of displacements by analyzing the phase differences of radar

signals between two SAR images with millimeter accuracy [67,69]. It can accurately determine both the amplitude and the phase of the microwave signal between two SAR image acquisitions, which are backscattered by the target. This type of radar interferometry allows a flexible choice of measurement geometry and spatial and temporal resolution [70]. The most common GB-InSAR technique for monitoring objects and terrain surfaces is differential interferometry. It allows precise measurement of displacements by analyzing phase differences between two or more radar acquisitions. The transmit and receive antennas' selectable location allows the angle of view to be optimized, adapting it to the surveyed area. As a result, monitoring accuracy and efficiency have increased. As with satellite techniques, GB-InSAR uses sensors operating in the X, C, and L bands. In addition, the system also has a Ku-band (1.67–2.5 cm), which has a frequency range of approximately 12 to 18 GHz [21], allowing for high spatial resolution images.

In recent years, GB-InSAR has been extensively used in landslide research, enabling improved monitoring and mapping activities [71,72]. It also allows the ability to accurately and precisely describe the deformation pattern, even in areas with different rates of displacement [73,74]. With its ability to select the appropriate measurement frequency, GB-InSAR technology overcomes the limitations of temporal decorrelation, which can be challenging in observing dynamic landslide processes [75,76]. In addition, it enables real-time or near-real-time monitoring of slopes [77,78], where it is necessary to take appropriate preventive measures due to rapidly developing displacements [67].

3.3. Optical, Multispectral, and Hyperspectral Imaging Overview

Recently, the launch of additional satellites into space, the thriving UAV market, and the increasing spatial resolution of the retrieved products have increased the use of optical, multispectral, and hyperspectral imaging techniques. Sensors mounted on satellites, aircraft, and UAVs use natural sunlight to record images of the Earth's surface in different spectral bands with varying spatial and temporal resolution. Optical systems operating allow for obtaining images similar to what the human eye sees. Multispectral and hyperspectral sensors capture images in several or even hundreds of selected spectral bands, i.e., near-infrared (NIR), shortwave infrared (SWIR), and Red Edge, which allow assessment of vegetation, soil, and hydrological conditions. For more detailed analysis, derived products, i.e., panchromatic images, panoramic sharpening, and false-color compositions, are also used to extract information on vegetation density, soil chemistry, and moisture.

In the case of satellite data, besides the crucial role of atmospheric conditions in data acquisition, the frequency of data collection is important, which depends on the satellite's revisit time. Figure 3 presents the most well-known satellites and information on the temporal and spatial resolution of the data they acquire. The most common satellites are Sentinel-2A and Sentinel-2B, which offer free access to data. Satellite platforms, such as WorldView and Pleiades, provide sub-meter maximum resolution images at daily intervals but still cannot match the spatial and temporal resolution of data acquired with UAVs, which are particularly useful for monitoring local land deformation and displacement [79,80].

Optical data were used to identify and map changes on the land surface, often relying on visual techniques [81,82], thereby providing valuable information on the history of deformation and the processes within them that affect slope stability [83–85]. Thanks to different spectral bands, using vegetation indices to monitor surface changes has proven to be an important element in providing essential information about environmental and morphological changes on the surface of the studied landslide areas [86]. These indices, such as the Normalized Difference Vegetation Index (NDVI) [52], the Normalized Difference Water Index (NDWI), the Soil Adjusted Vegetation Index (SAVI), and the Normalized Multiband Drought Index (NMDI) [53], are calculated based on different spectral channels, allowing us to assess the condition of vegetation and identify areas that are changing over time.

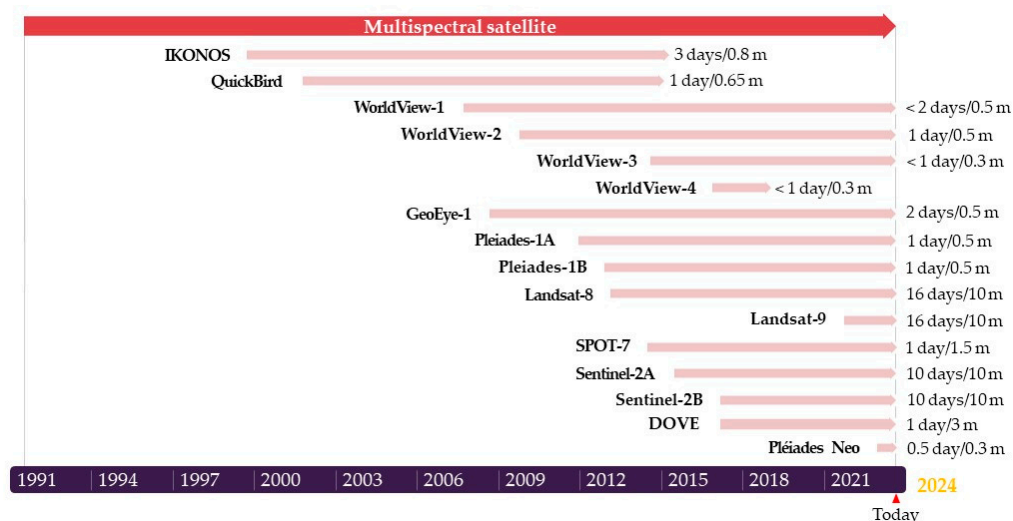


Figure 3. Selected active optical satellites used for terrain monitoring; modified after [21], licensed under CC BY 4.0.

3.4. LiDAR Overview

LiDAR is a remote, three-dimensional (3D) measurement technology using laser light. It sends a laser pulse from the instrument to the object's surface and back to the detector. The distance between the instrument and the object is calculated by measuring the phase difference in the signal or the time course of the measurement pulse while recording the laser beam's horizontal and vertical deviation angles [87]. LiDAR systems can be mounted on mobile platforms (airborne laser scanning (ALS) with regional coverage) or placed on tripods on the ground (terrestrial laser scanning (TLS) with local coverage). It is also increasingly common to see laser scanners mounted on UAVs, walking robots, or autonomous vehicles.

In recent years, most sensors have been dominated by linear mode LiDAR (LML), with a single wavelength and a single pulse, with the possibility of single- or multi-pulse operation. Recently, however, several new LiDAR technologies and sensors have emerged, such as multi-pulse in the air (MPiA) LiDAR, full waveform digitization (FWD) LiDAR, multi-spectral LiDAR (MSL), Geiger Mode LiDAR (GML), and Single Photon LiDAR (SPL) [88]. Each has unique features and applications, allowing the appropriate sensor selection for specific needs.

The most common LiDAR sensors record one to three features of the reflected pulse. In contrast, modern sensors can register up to a dozen echoes, depending on the laser scanner and the surface from which the signal is reflected [89]. In addition, full-waveform LiDAR systems can record the entire waveform of the return pulse, enabling the identification of different structures and objects in the surveyed area. This allows these systems to penetrate even dense vegetation, providing details on the canopy, sub-canopy structures, ground vegetation, and ground morphology [2].

TLS and ALS techniques are generally used to monitor unstable slopes [90,91], debris flows [92], and slow-moving landslides [93] and to create digital elevation models (DEMs) even in areas with high vegetation cover [94]. Models created based on TLS are compared with products obtained in previous measurement series to determine displacements for individual landslides [2]. In contrast, ALS is mainly used for landslide inventory and mapping [95,96]. TLS and ALS also allow the estimation of changes in the volume of removed and/or accumulated material, allowing the identification of landslide sites and their evolution over time [97,98]. In recent years, the potential of point cloud correlation techniques for monitoring the displacements of active landslides has also been explored. The results have shown that these methods are particularly useful for observing areas with small surface changes [99,100]. However, by supplementing the research with further geospatial

techniques, such as discontinuity line tracking, it is possible to detect displacements of several meters [101].

3.5. IRT Overview

IRT is a technology based on acquiring and processing information about the infrared radiation emitted by objects. This type of measurement is performed using non-contact devices such as thermal imaging cameras and infrared cameras [102]. The acquired data are converted into visible images by assigning the appropriate infrared energy level to the pixels. This results in images called thermograms [103]. In the case of ongoing research, radiant temperature maps are obtained after prior correction of sensitive parameters, i.e., object emissivity, path length, air temperature, and humidity [21].

In research using the IRT technique, observations of the areas under investigation are carried out from satellite, aerial, or ground levels. Currently, several satellites are acquiring thermal data from different regions of the earth. These include Landsat, which is used to monitor forested areas; the Moderate-Resolution Imaging Spectroradiometer (MODIS), which monitors forested areas and water quality; Sentinel-3, which allows monitoring of ocean and land surface temperatures; and Geostationary Operational Environmental Satellites (GOES) with a thermal imaging camera, which allows monitoring of atmospheric conditions. Thermal imaging cameras mounted on aerial platforms such as drones or aircraft enable thermal imaging measurements over much smaller areas. However, they enable more detailed identification of areas with different thermal properties. IRT analysis can be approached in two ways. The passive approach utilizes the natural thermal radiation emitted by the objects under investigation, mainly for monitoring surface temperatures and detecting warm and cold areas on objects. In contrast, the active approach requires an external energy source to induce the appropriate thermal contrasts.

IRT is increasingly being used to characterize and map unstable slopes. To achieve a more accurate and detailed interpretation of the results, IRT is typically integrated with other RSTs, such as TLS and GB-InSAR [21]. This integration allows for detecting rock mass cracks, subsurface voids, and moisture and seepage zones. Their formation affects the thermal properties of the medium, i.e., density, heat capacity, or conductivity, and these changes can be detected on the created temperature maps as thermal patterns that differ from the surroundings [104]. Such areas are called thermal anomalies and can indicate potential slope instability [90].

3.6. Temporal Evolution of the Scientific Production

In this review, 165 articles, spanning from early 2010 to early January 2024, were analyzed and statistically compiled (Figure 4a). The distribution of the described RSTs in the articles analyzed over the years is shown in Figure 4b. It should be noted that several different measurement techniques were used in many of the articles. Therefore, the numerical values in Figures 2, 4b and 5 do not add to those in Figure 4a.

In the initial period, the number of publications using RSTs gradually increased. However, a significant increase occurred in the second half of the study period, which was attributed to the development of satellite and aerial technologies, global data availability, and increased public awareness.

The first publications using RSTs to study landslide precursors, dating from the beginning of the review period (2010–2012), used techniques such as GB-InSAR, LiDAR, and optical imagery. In addition to the data during this period being mainly acquired from the ground level, a few articles using satellite precipitation monitoring systems were also classified as ‘others’ (Figure 4b) [105]. Publications from the beginning of the study period were mainly focused on supporting the monitoring and early warning of unstable slopes from ground level. Landslide monitoring using satellite and aerial data became increasingly popular over the review period, especially in 2016–2023, caused by access to data from newly launched radar and optical satellites, i.e., ALOS, Sentinel-1, Sentinel-2, and TerraSAR-X (Figure 4b).

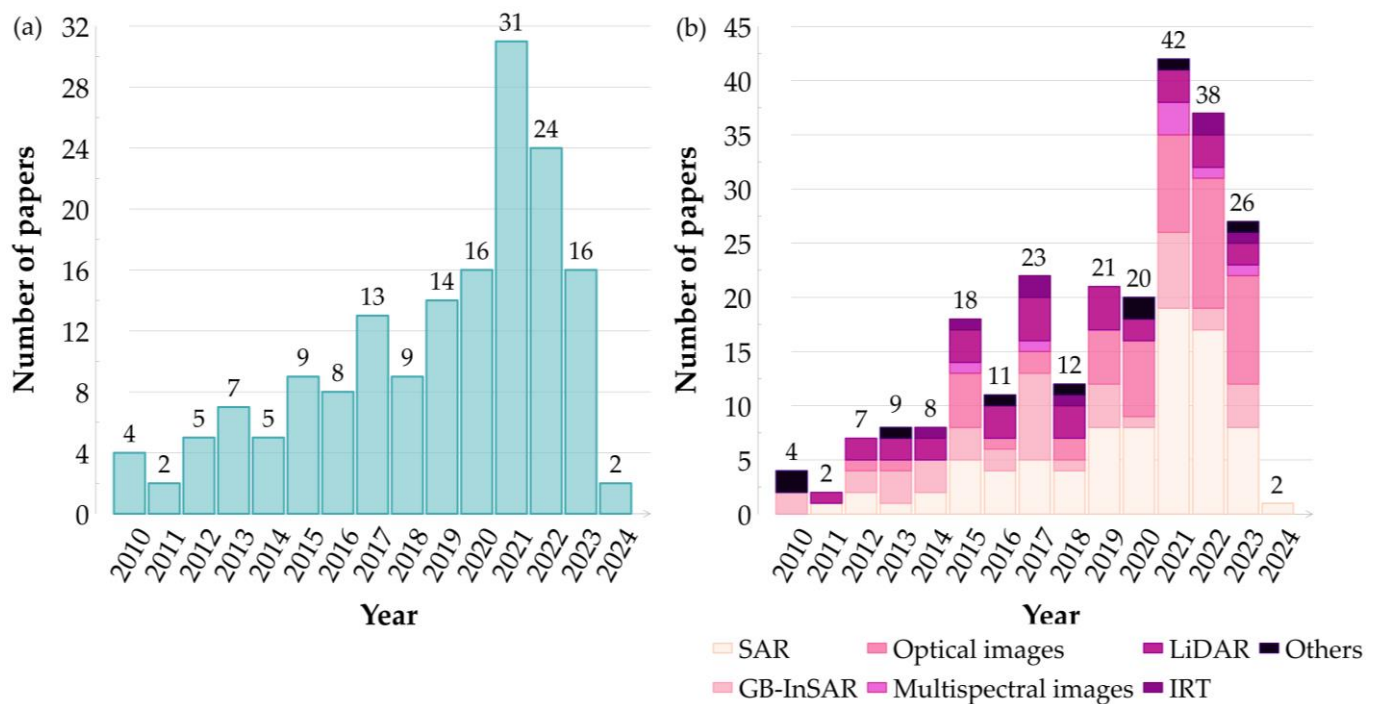


Figure 4. Selected scientific articles on RSTs published between 2010 and 2024. Figure (a) shows the distribution of the selected 165 articles over time. Figure (b) shows the number of articles describing each RST in different periods.

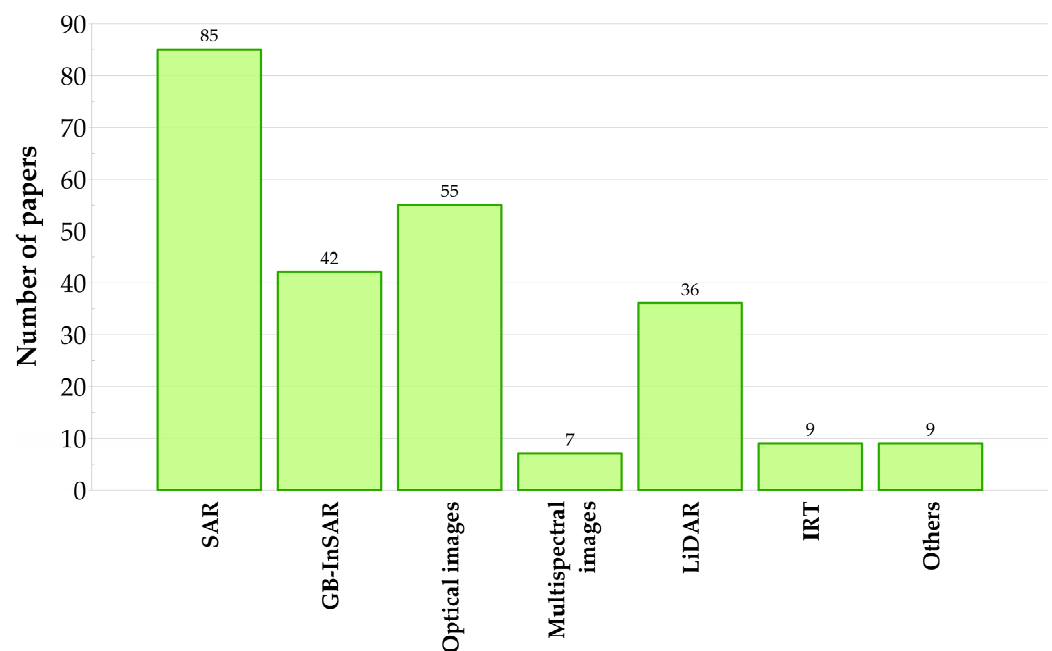


Figure 5. Number of articles in the review using different types of RST in research.

Figure 5 shows the quantitative distribution of articles that used different RSTs between 2010 and 2024. As many as 85 articles describe the use of SAR in their research, indicating its popularity in landslide precursor studies.

SAR, associated with various techniques (Figure 6a), has become essential due to its independence from atmospheric conditions and the possibility of using current and historical data in the analyses. In particular, its significance is noticeable due to the increasing number of articles using the MT-InSAR technique in research, allowing deformation to

be monitored over time (Figure 6b). This enables a better understanding of the processes' dynamics and the identification of deformation patterns and trends. Despite the emergence of more advanced technologies, GB-InSAR is still prevalent due to its high accuracy and ability to monitor ground deformation in real-time, as confirmed by 42 articles utilizing this technique. The emergence of drones and improved optical, multispectral, and hyperspectral sensors have contributed to significant advances in detecting displacements and deformations on the ground surface. Improvements in the quality of satellite data have made it possible to identify and study temporal changes on the ground surface with magnitudes as small as a few tens of centimeters [106]. In addition, advances in computerization have enabled the development of algorithms that automatically determine displacements based on images, as confirmed by as many as 62 articles describing the use of these techniques in research. Among the 36 articles in the review that use the LiDAR technique, most describe the use of point clouds, acquired with this technique, to monitor landslide-prone areas. LiDAR products are characterized by high spatial resolution and the ability to create 3D models, which has made the technique popular for landslide monitoring and EWSs. Meanwhile, publications using IRT to identify landslide precursors have shown that the ability to analyze significant thermal changes may play a crucial role in future landslide research. These features are important in permafrost regions, where freeze–thaw cycles and snowmelt caused by elevated temperatures affect the stability of the land surface [83].

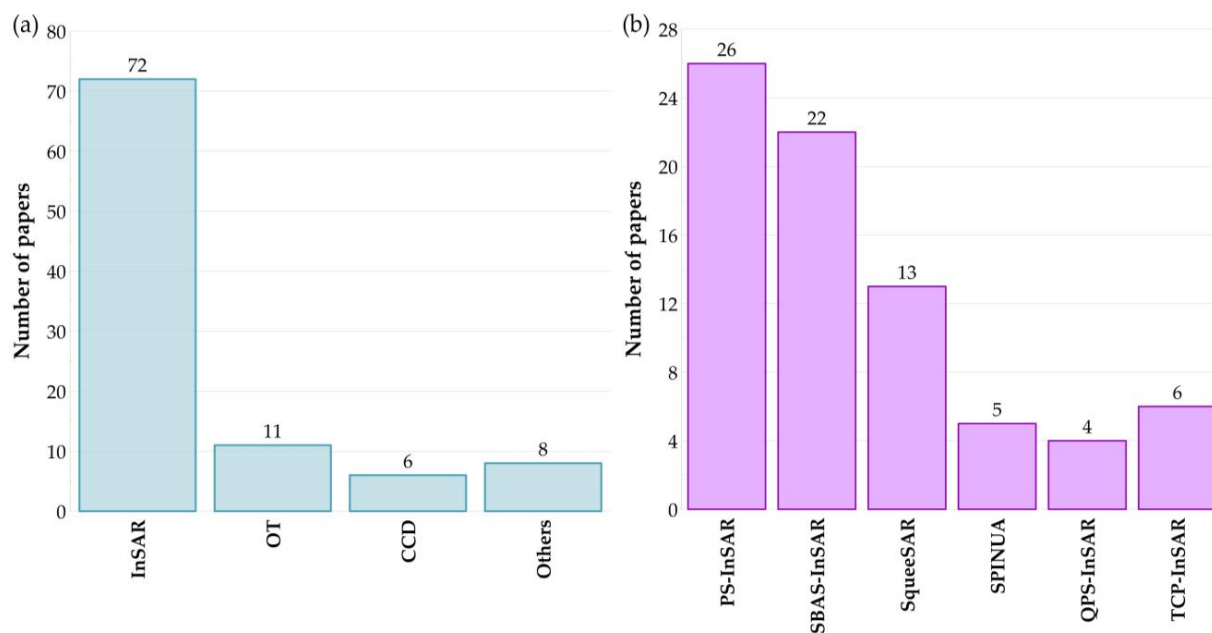


Figure 6. (a) The number of articles analyzed describing the use of SAR techniques; (b) the number of articles using MT-InSAR techniques in these studies.

4. Application of RSTs in Landslide Precursor Detection and Measurement Data Integration in EWSs

Landslides, especially those of large magnitudes, can indicate early warning signals involving geomorphological, geotechnical, and geoenvironmental precursors [83]. These mainly include changes in terrain, vegetation, hydrology, and cracks and fissures. Detecting the precursors of landslides offers the possibility of early identification and warning long before they occur. RSTs, enabling remote monitoring of areas in a regular and systematic manner, are a powerful tool with great potential to achieve this goal. However, this requires analysis to determine what precursors may be typical of a landslide, depending on the type of landslide (fall, topple, slide, spread, flow), the degree of activity (active, dormant, or potential), and what mechanisms may trigger it (precipitation, earthquakes, human activity, hydrological changes, melting glaciers, and snow) [107]. When creating EWS on a regional scale, where the genesis of landslide formation and types of landslides may

differ, it is necessary to look for the most optimal solution that integrates appropriate measurement techniques. Therefore, in order to create an effective EWS, it is essential to integrate appropriate measurement techniques, taking into account the specific geological and climatic characteristics of the region, which will enable effective monitoring and analysis of potential landslide hazards.

This section of the article discusses the types of landslide precursors identified by RSTs, such as coherence changes, cracking, displacements, temperature, structural discontinuities, and vegetation indices (Table 2). Based on the literature review, methods for integrating RSTs into landslide monitoring and EWSs are also presented.

Table 2. Landslide precursors detected by various RSTs.

RST		Precursor Type	
SAR	CCD	<ul style="list-style-type: none"> displacements [3,28,31,83,108] coherence changes [26,109,110] 	Figure 7
	OT		Figure 8
	InSAR		Figure 9
GB-InSAR		<ul style="list-style-type: none"> displacements [68,78,111,112] 	Figure 10
Optical images		<ul style="list-style-type: none"> displacements [113] structural discontinuities [83] 	Figure 11
Multispectral/Hyperspectral images		<ul style="list-style-type: none"> vegetation indices change [109] 	Figure 12
LiDAR	ALS	<ul style="list-style-type: none"> displacements [114–117] cracking [114,118] 	Figure 13
	TLS		Figure 14
IRT		<ul style="list-style-type: none"> temperature [54,83,119] 	Figure 15

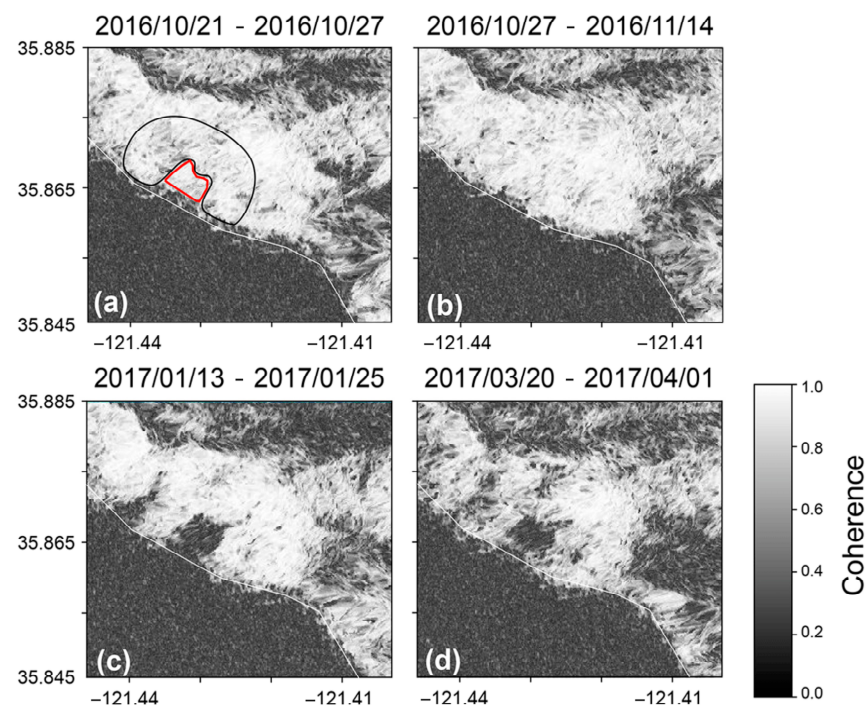


Figure 7. Interferometric coherence of the Mud Creek landslide in California (USA), outlined in red, and the surrounding reference slope, outlined in black. Figures (a,b) show the slope in autumn 2016, while figures (c,d) show the loss of coherence in this area in spring 2017. The landslide occurred on the 20th of May 2017; modified after [109], licensed under CC BY 4.0.

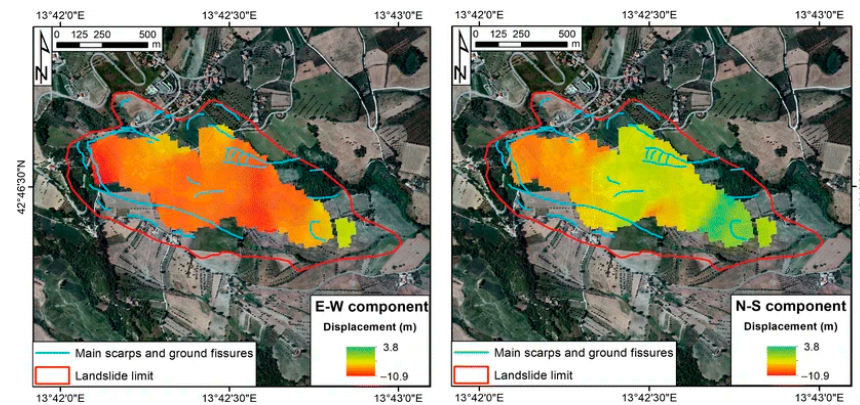


Figure 8. Rapid motion tracking results for the landslide area in Ponzano (Italy), East–West (range), and North–South (azimuth) components; source [28], licensed under CC BY 4.0.

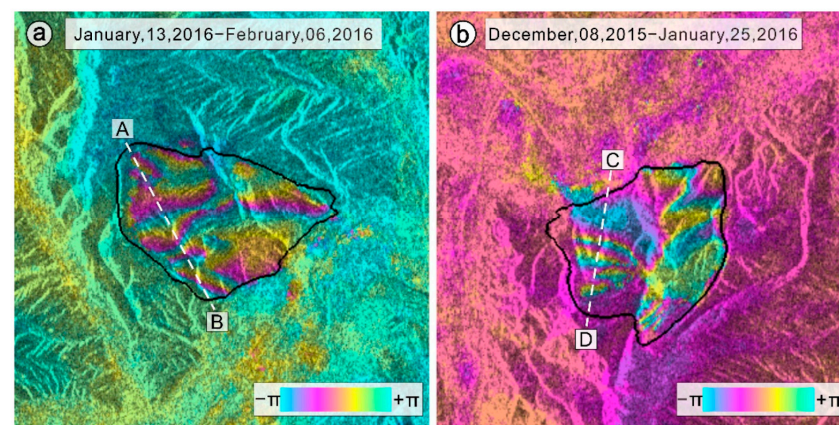


Figure 9. Differential interferograms in the radar coordinate systems for the Gaojiawan landslide (China), created from Sentinel-1A (a) ascending and (b) descending images. The segments from point A to point B (a) and point C to point D (b) designations illustrate where distinct color changes were observed in the interferograms, corresponding to large ground displacements in these areas; source [31], licensed under CC BY 4.0.

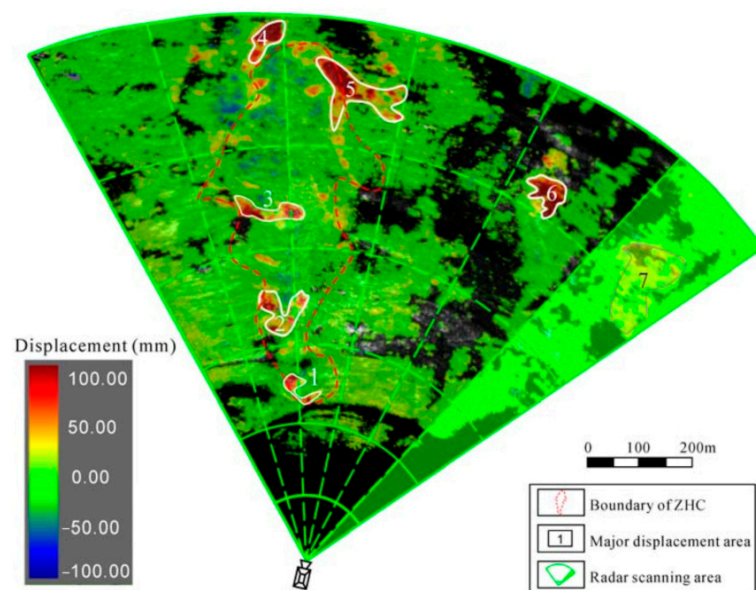


Figure 10. Cumulative displacement map was obtained from measurements taken shortly before the Zhonghaicun landslide in southwest China on 21 and 22 September; source [111], licensed under CC BY 4.0.

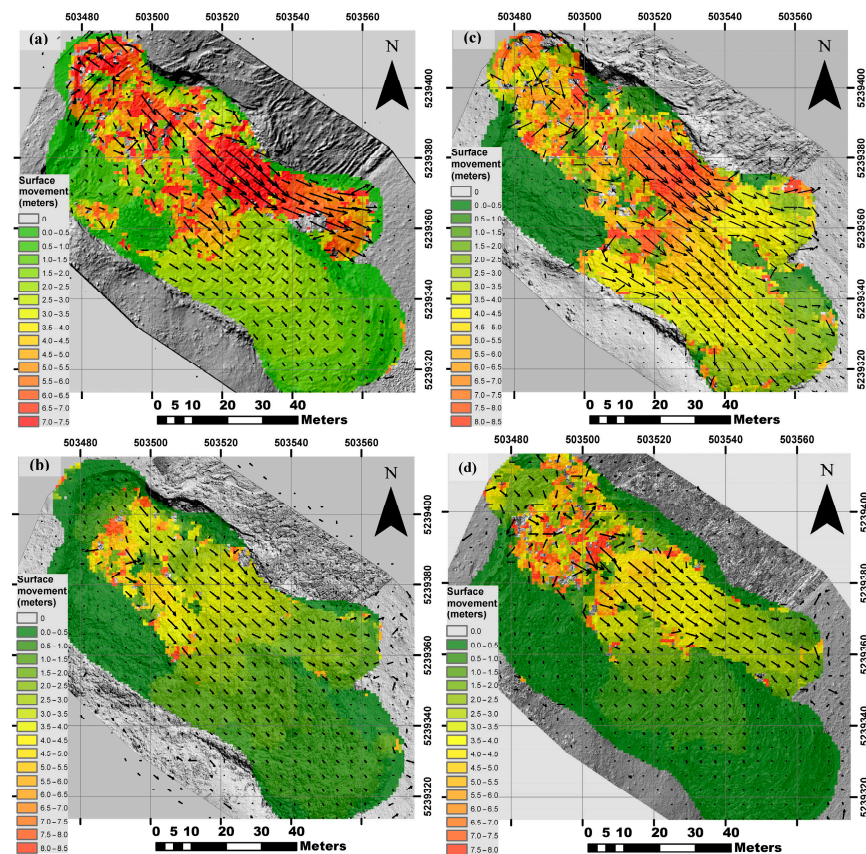


Figure 11. Surface movement maps determined from correlations of RGB images between annual data sets for the Home Hill landslide (Tasmania, Australia); (a) 2011B–2012A; (b) 2012A–2013A; (c) 2013A–2013B; (d) 2013B–2014A. The black arrows show the direction and size of the displacements; modified after [113], licensed under CC BY 4.0.

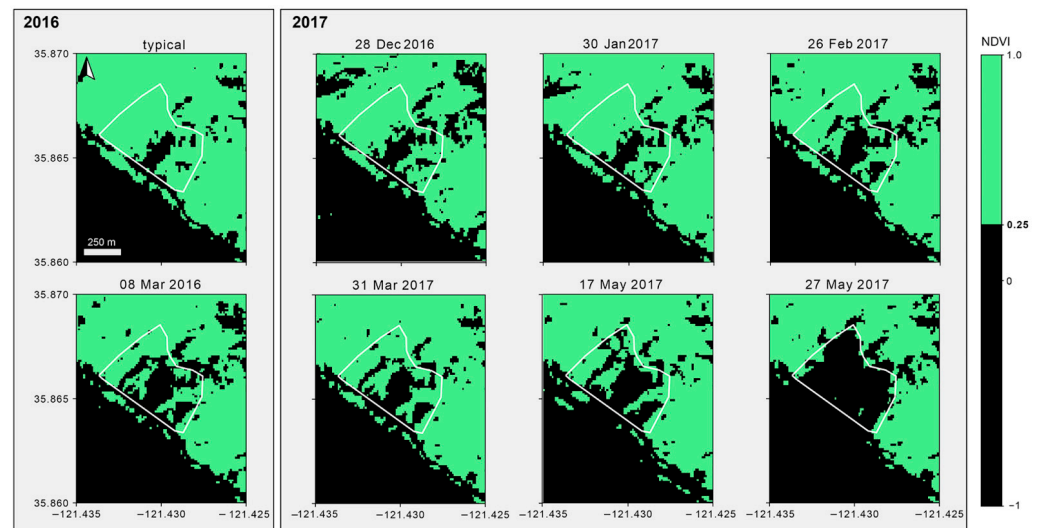


Figure 12. Analysis of NDVI in the Mud Creek landslide area. The first panel depicts the typical vegetation behavior pattern. The second one corresponds to the dip in the NDVI index observed in early 2016, which grew more significant during the spring of 2017, before most of the vegetation was removed due to the landslide that occurred on the 20th of May 2017; source [109], licensed under CC BY 4.0.

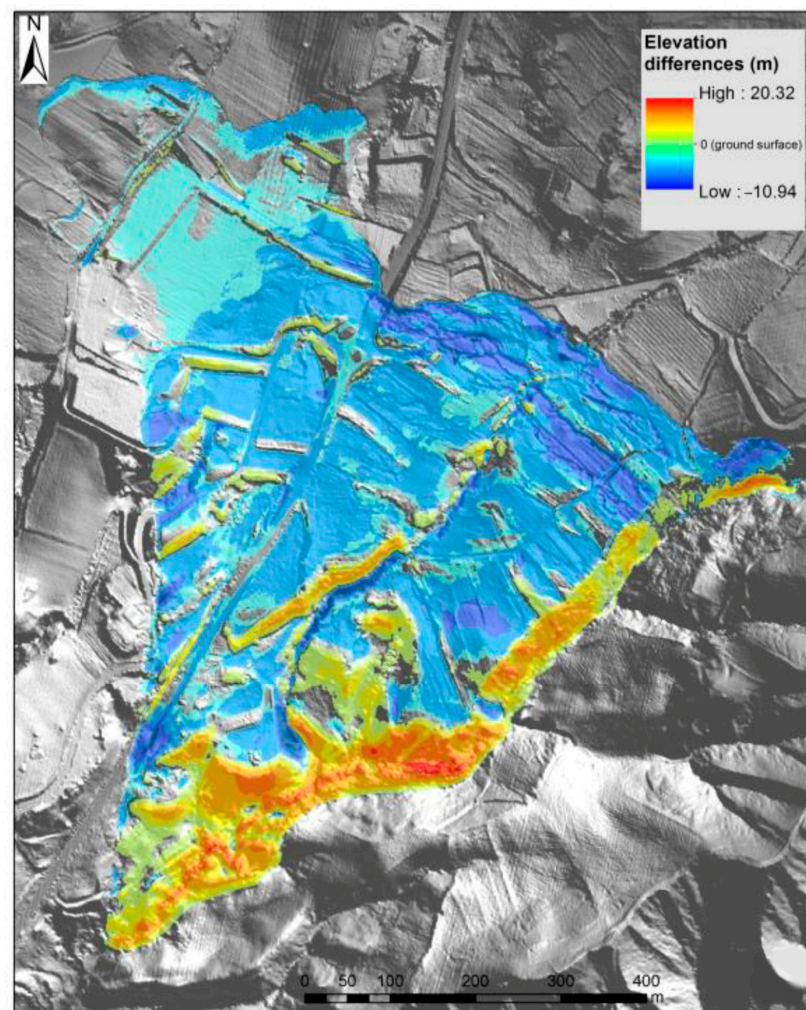


Figure 13. Spatial distribution of the elevation differences, obtained by subtracting the DEMs for the Montescaglioso landslide; modified after [114], licensed under CC BY 4.0.

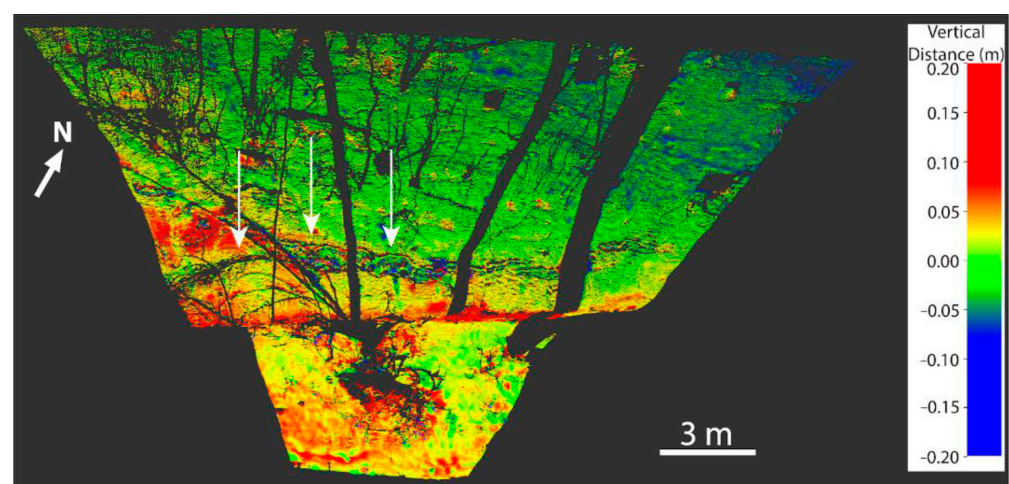


Figure 14. The differences between point clouds for the landslide in Kechries (Greece) were obtained from TLS in August 2020 and March 2021; source [118], licensed under CC BY 4.0.

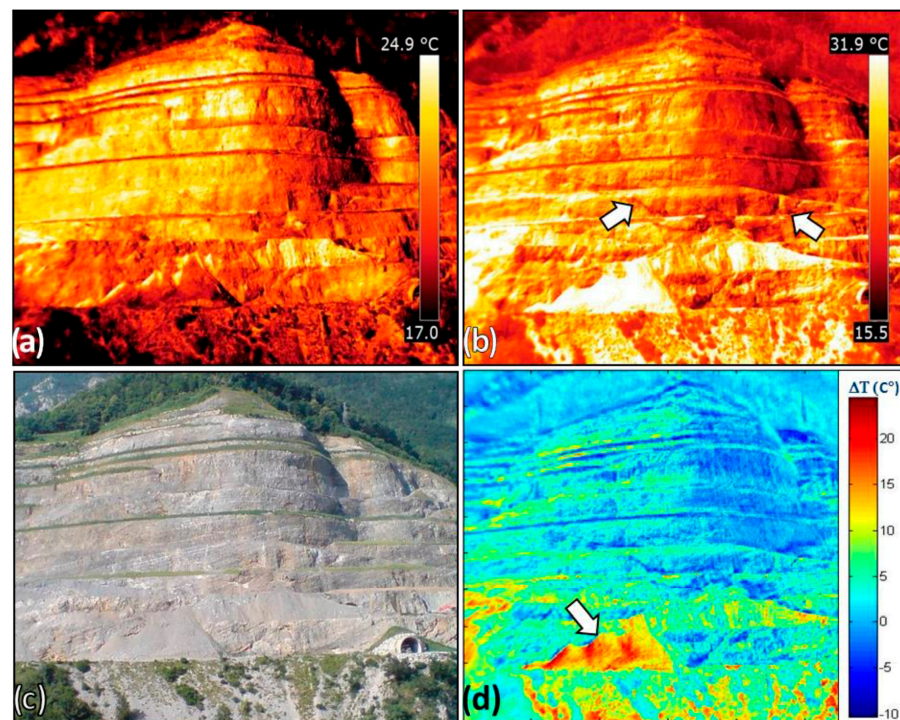


Figure 15. Temperature maps of the studied surface of the Roaschia (Italy) rock slide were acquired at 8:00 a.m. (a) and 1:00 p.m. (b). The arrows in image (b) indicate cold thermal anomalies that are undetectable in the corresponding optical image acquired by a built-in digital camera (c). The arrow on the generated differential surface temperature map (d) indicates thermal variations on the slope surface, signifying higher heat transfer capacity than the surrounding rocks; modified after [119], licensed under CC BY 4.0.

4.1. SAR Techniques

The current development of SAR techniques, access to increasing high-spatial and temporal resolution data, and the ability to acquire data from large areas have also made this technique widely used in landslide monitoring, enabling precise monitoring of millimeter-scale deformations. The ability to analyze changes in soil structure, decreases in interferogram coherence values, the velocity of the resulting deformations, and their acceleration over time provide the basis for this technology to be widely used in the study of landslides and the identification of their precursors.

One of the most straightforward techniques for detecting disturbing changes in the ground surface is SAR data analysis using coherence change. Although it is a statistical value and does not allow for the determination of specific displacement values, it allows the detection of areas where there has been a change in its value over time [110]. A high value usually indicates ground stability, while a decrease may indicate displacements or changes in the ground structure, as occurred during the studies conducted at the Mud Creek landslide [109]. The authors of the article used radar images acquired from the same path to minimize the influence of spatial decoherence. However, the problem of temporal coherence loss was solved by using an improved CCD technique to assess ground deformation and land cover changes caused by landslide activity. By calculating the ratio of the average coherence of the surrounding slope to the average coherence of the landslide itself, it was possible to eliminate disturbances caused by temporal loss of coherence, weathering, and vegetation cycles. Thus, it was possible to detect a significant decrease in coherence due to temporal and spatial decorrelation in an area that had suffered a landslide as much as five months before the disaster occurred. Despite the significant potential of this precursor, additional research is needed to determine which types of landslides exhibit this kind of behavior and how much deviation from the stable indicators indicates

instability. Another successful application of the CCD technique for landslide detection is using coherence difference and normalized coherence difference indices [26]. To eliminate the impact of phase decorrelation, vegetation covering the studied areas was reduced by calculating NDVI values from Sentinel-2 satellite images and creating an NDVI mask with a threshold considered the boundary between areas with bare soil and low vegetation. As a result, maps of pixels classified as landslide or non-landslide areas were created, enabling the determination of optimal decision thresholds and the identification of areas potentially at risk of landslides. However, problems resulting from the overgrowth of landslide areas with high vegetation still appear to be a significant obstacle to the precise monitoring and search for landslide precursors.

Developments in SAR techniques have made it possible to conduct advanced applications of MT-InSAR techniques for monitoring not only individual landslides but also deformation on a regional scale. While the SqueeSAR technique allowed for the detection of a trend change two years before the event in Ponzano [28], which can be seen as a precursor to the main failure of the monitored landslide, the use of MT-InSAR to detect and measure ground movements on a large scale faces several challenges [120]. In the case of the system described in the paper, these include image decorrelation in vegetated areas, low spatial resolution, and ambiguity in the precise location of measurement points on a meter scale. The OT technique has also been used to evaluate the deformation field caused by the Ponzano landslide [28]. While the technique can determine displacements of tens of centimeters to several meters, it also has huge potential for identifying precursors by detecting the acceleration of active landslides.

In Italy, a system for monitoring and mapping landslide-prone areas based on the systematic processing of Sentinel-1 data using the SqueeSAR technique has also been developed for the Tuscany region, providing a continuous flow of processed data [42]. The described approach was carried out in search of anomaly points indicating a change in movement dynamics. However, once a change in the deformation pattern is detected, it must be analyzed and correctly interpreted to decide whether the anomalous pattern is consistent with the actual slope dynamics. Therefore, the interpretation of SAR data alone is not sufficient. It requires proper analysis supported, among other things, by information obtained from various types of topographic, geomorphological, and geological maps, as well as in situ data that can attribute geomorphological significance to scattered ground displacement measurements at individual points. A similar approach was used in a study applied to the central part of the Three Gorges Reservoir area (China), in which InSAR techniques were used on a regional scale to identify precursors and active landslides or zones of major deformation that required further investigation [3]. The current strategy has great potential to expand the existing system by integrating various RSTs to analyze potential landslides in detail, significantly reducing the workload.

4.2. GB-InSAR Techniques

GB-InSAR has significant potential for detecting landslide precursors due to its ability to quickly process and interpret data in near-real time, enabling the detection of signals indicating impending hazards. Possible delays before issuing a warning, resulting from the need to analyze the acquired data, do not pose a problem for landslides characterized by slow or moderate velocity.

The ability to detect even the smallest changes on the ground surface using GB-InSAR enables the detection of microdeformations. This was the case with the detection of a secondary landslide in Zhonghaicun (China), triggered by heavy rainfall that accelerated over time, leading to a landslide [111]. The L-band synthetic aperture radar (MDSR-LSAR) carried out enabled near-real-time recording of cumulative displacement time data in the landslide area and the surrounding region. The velocity of the earth masses and the velocity increment exceeded the alarm threshold, resulting in the automatic transmission of an alarm message. The displacements and their increase over time detected with GB-

InSAR have proven to be useful precursors to avoiding another disaster. Unfortunately, in hard-to-reach areas, conducting such surveys can be very difficult or even impossible.

Another approach exploiting the potential of GB-InSAR to detect precursors to actual slope displacement was also described in a paper on monitoring a gradually moving landslide [112]. The developed system detected ground surface displacement towards the bottom of the slope based on differences in the phase of the radar signal. It made monitoring displacements of different velocities over the entire analyzed area possible. However, the developed system does not have the ability to detect displacements in the acceleration phase of a landslide, which is the essence of support for EWSs.

4.3. Optical, Multispectral, and Hyperspectral Imaging Techniques

Using optical, multispectral, and hyperspectral data acquired from different altitudes with appropriate revisit times has become an essential source for acquiring landslide precursors such as displacements, structural discontinuities, and changes in vegetation indices. Depending on the type of landslide and its patterns of change, precursors detected by optical images can appear from days to months or even years before the event [121,122]. The case of monitoring the Trièves area in the Western Alps (France) enabled precursor motions to be detected three days before rapid landslides based on optical images (Sentinel-2, Landsat-7/8) [14]. Growing areas of exposed slopes, which are visual precursors of landslides, allowed the detection of area changes exceeding 10,000 m² in 5 years [39], which gives a good chance of identifying sites potentially at risk of landslides over vast areas. Multi-temporal optical images are also used to investigate potential geomorphological precursors of large ones, such as large cracks, escarpments, and rock slides [106]. Visual interpretation based on them showed that the detected geomorphological features were correlated with available slope deformation data, which supports the idea that they may be geomorphological precursors of rock slides. Visual analysis of optical imagery is very useful as a first step in identifying potential landslide areas due to detecting vegetation changes even months before a landslide occurs [123]. However, quantitative analysis of ground displacement values, which usually requires more sophisticated measurement techniques, is more important to detect their precursors. This is because they can provide more precise information for landslide risk assessment.

This data type can be provided using high-resolution remote sensing images and the scale-invariant feature transformation (SIFT) algorithm to monitor intense landslide displacements [124]. SIFT is an algorithm for determining the displacement vector field based on matching invariant features against image transformation, rotation, zooming, and affine transformation. Continuous monitoring of the displacement of active landslides is also based on high-resolution optical images analyzed using cross-correlation algorithms [125]. COSI-Corr is one of the most widely used tools that allows precise time series registration of optical satellite and aerial images and sub-pixel measurement of landslide surface displacements [113,126,127]. Cross-correlation, which enables real-time analysis of slope movement, has also been used to apply flow visualization techniques using time-lapse imagery (TLI). The acquisition of slope motion velocity vectors is achieved using particle image velocimetry (PIV) algorithms [128]. As a result of ongoing monitoring, slope movement initiated by rainfall 20 days before the landslide occurred was recorded. The image correlation technique is more robust to vegetation's influence than InSAR data but requires images from the same season [126].

The development of UAV photogrammetry and the drive for automation have made it possible to develop a landslide monitoring system that acquires data automatically and then enables the creation of point clouds and 3D models of the study area [129]. Such a system, based on the comparison of current data with results from previous series, allows the status of landslide activity to be monitored in a short period of time [130]. However, this type of solution encounters the resulting dependence of the measurements on weather conditions and the limited measurement range (1–2 km).

Multispectral data, covering several to hundreds of spectral channels, can provide more detailed information on the condition of the vegetation present in an area, the moisture content of the soil, or its chemical composition. An approach using multispectral data to study the precursor to a change in the NDVI index in assessing landslide activity allowed the time series of the index to be calculated as the ratio of the average NDVI in the area considered unstable to the surrounding slope [109]. The advantage of the proposed approach was the elimination of disturbances due to temporal loss of coherence and the negative impact of disturbances due to weathering and vegetation cycles. The developed technique proved to be a very useful precursor for the landslide, as it showed that the NDVI decreased almost linearly five months before the landslide occurred. Unfortunately, further research is required to assess the feasibility of using the proposed solution for heavily vegetated slopes and to determine how much deviation from stable indices indicates slope instability.

4.4. LiDAR Techniques

LiDAR is a technique for detecting precursors such as displacements and cracking [114,116,117]. In the case of determining land surface displacements, it usually involves comparing point clouds or creating digital terrain models (DTMs) between measurement series. Although the data acquisition technique does not differ significantly, the method of processing the acquired data, depending on the type of area under study and the expected results, plays a significant role.

When dealing with small displacements, identifying precursors to potential landslides can be challenging due to the limited accuracy of the equipment or observation techniques used, which can be crucial. In one article, using TLS to monitor slow-moving landslides, a hybrid-weighted iterative closest point (HWICP) algorithm and an adaptive local cloud-to-mesh method (ALC2M) were used to detect precursors of small deformations [115]. The algorithms used enabled the precise unification of spatial references in long-range TLS point clouds from different epochs and the eventual detection of deformations in the monitored objects. The obtained results demonstrated the ability and potential to detect small deformations before the failure of slow-moving landslides within the Three Gorges Reservoir Region (China) with complex topography.

Using TLS to detect new cracks and monitor scarps of pre-existing landslides allows mapping deformations and changes on the land surface with high spatial resolution, which can be used as a precursor to landslides [114,118]. Detected changes can be the first step in taking preventive measures and making detailed observations of areas where significant changes have occurred. However, due to the limitations of observing individual landslides, it is suggested that other measurement techniques be used, which require much less effort and are less costly [118].

4.5. IRT Techniques

IRT enables the identification of landslide precursors by monitoring a time series of geoenvironmental information, such as thermal changes. The technique is particularly effective in permafrost regions, where landslides are caused by freeze–thaw cycles and snow melt, affecting surface stability.

Thermal sensors operating at the satellite level can collect ground temperature information on a regional scale, which can significantly support EWSs. Inversion analyses of ground surface temperature and soil moisture were carried out using IRT to reflect the actual conditions of the monitored region near Beihei Highway (China) [54]. Ongoing monitoring and measurements based on discrete points allow macro-regional environmental changes to be captured and the evaluation of the unstable region to be carried out. The study results show they can support assessment and early warning of significant deformations caused by climate change and permafrost degradation. Limitations of temporal and spatial resolution for frequent measurements may require other techniques.

The data used in the time series analysis of the thermal environment for the Pink Mountain, Mount Meager, and Yigong landslides, located high in the mountains, showed an increase in the temperature of the monitored areas before the occurrence of each event [83]. The proposed approach to detecting precursors is limited to only glacial and snowy areas, which poses a problem when monitoring landslides in different locations.

Landslide mapping using IRT may also be useful in detecting landslide precursors [119]. The thermal anomalies revealed indicate the ability of IRT to identify signals indicating unstable areas such as faults and sediment cones. However, by mapping the obtained results onto a 3D differential map of the surface acquired with TLS, integrating the techniques can significantly facilitate the interpretation of the data and identification of potentially unstable areas.

4.6. Measurement Data Integration in EWSs

A deeper understanding of landslide processes' failure mechanisms and dynamics is required to effectively apply appropriate monitoring instruments and techniques (classical and remote sensing). Classical in situ measurements, which include such sources of information as surveying, geotechnical, geophysical, and hydrological measurements, provide detailed information at the local level. Because of their ability to acquire comprehensive data remotely from wide areas, RSTs are increasingly favored in EWSs.

This section presents the various measurement techniques used in EWSs to monitor landslides and detect their precursors (Table 3). The first section describes systems that integrate both classical and RSTs. They enable continuous monitoring and tracking of landslide evolution history, mapping of landslide activity, and analyzing development trends, significantly reducing the risk of landslides [131]. The second part presents case studies that examine the use of RSTs alone to monitor and detect landslide precursors. It also presents the possibility of overcoming the limitations of applied RSTs by using other RSTs.

Table 3. Landslide monitoring techniques relating to landslide type and parameters to monitoring.

Landslide Type	Parameters to Monitoring	Equipment for Monitoring	Monitoring Techniques	Reference
Multidisciplinary approaches				
Rock slides	Displacement, Deformation, Volume calculations, Inclination, Rainfall, Temperature	Ground radars, Laser scanners, UAVs, GNSS receivers, Cameras, DMS instrumentations, Extensometers, Tiltmeters, Rain gauges, Thermometers	GB-InSAR, LiDAR (ALS, TLS), UAV photogrammetry (3D modeling analysis), GNSS measurement, Deformation analysis, Geotechnical measurements using extensometers and tiltmeters, Rainfall monitoring, Temperature monitoring in boreholes and modeling	[132]
Rock slides	Displacement, Deformation, Rainfall, Crack features	Radar satellites, UAVs, GNSS receivers, Crack meters, Rain gauges	InSAR, UAV photogrammetry (3D modeling analysis), GNSS measurement, Geotechnical measurements using a crack meter, Rainfall monitoring	[133]
Translational slides	Displacement, Inclination	Radar satellites, Inclinometers	InSAR (PS-InSAR, DS-InSAR), Geotechnical measurements using inclinometer	[134]

Table 3. Cont.

Landslide Type	Parameters to Monitoring	Equipment for Monitoring	Monitoring Techniques	Reference
Earth flows	Displacement, Deformation, Detecting the sub-surface structure of landslides, The distribution of hydrological characteristics and reconstructing the landslide body	Radar and optical satellites, Laser scanners, Multi-electrode resistivity meters	InSAR (SBAS-InSAR), Optical image analysis, TLS (3D modeling analysis), Geophysics measurements using ERT	[135]
Rock slides	Displacement, Vibration	Radar and optical satellites, Seismic stations	InSAR (D-InSAR), Optical images and DEM analysis, Monitoring seismic activity	[136]
Lateral spread	Displacement, Deformation, Inclination	Radar satellites, UAVs, GNSS receivers, Extensometers, Tiltmeters	InSAR (PS-InSAR), UAV photogrammetry (3D modeling analysis), GNSS measurement, Geotechnical measurements using extensometers and tiltmeters	[137]
Deep-seated landslides	Displacement, Deformation, Atmospheric conditions, Groundwater level, Visual change detection	Radar satellites, Ground radars, UAVs, Automatic weather stations (AWSs), Wireless networks, Camera systems (PICs)	Mobile techniques: InSAR (SBAS-InSAR), GB-InSAR, UAV photogrammetry (3D modeling analysis, orthomosaic analysis), Permanent techniques: Meteorological data analysis, Groundwater level measurements, Optical images analysis	[138]
Slow moving landslides	Displacement, Deformation, Inclination, Rainfall	Radar satellites, Inclinometers, Extensometers, Rain gauges	InSAR (PS-InSAR), Geotechnical measurements using inclinometer and extensometers, Rainfall monitoring	[139]
Remote Sensing approaches				
Flows	Displacement, Deformation, Change detection	Radar and optical satellites, UAVs	InSAR, Optical images and aerial images analysis	[50]
Different types of landslides	Displacement, Deformation, Creep	Radar and optical satellites, UAVs	InSAR, Optical images and aerial images analysis	[20]
Rockfalls, Rock slides	Displacement, Deformation, Temperature	Ground radars, Laser scanners, Thermal cameras	GB-InSAR, TLS (point cloud and 3D modeling analysis), IRT (temperature map analysis)	[58]

Table 3. Cont.

Landslide Type	Parameters to Monitoring	Equipment for Monitoring	Monitoring Techniques	Reference
Mud flows	Displacement, Coherence change detection, Vegetation index, Rainfall, Temperature	Radar and optical satellites, Rain gauges, Thermometers	InSAR (NSBAS—the new small baseline subset), CCD, Multispectral images, Rainfall and temperature monitoring	[109]
Rockfalls	Displacement, Deformation	Radar satellites, Ground radars, Laser scanners	InSAR (PS-InSAR), GB-InSAR, TLS (3D modeling analysis)	[108]
Translational slides	Displacement, Deformation	Radar satellites, Ground radars	InSAR (PS-InSAR), GB-InSAR	[140]
Earth flows	Displacement, Deformation, Change detection	Radar satellites, UAVs	InSAR (SBAS-InSAR), UAV photogrammetry (3D modeling analysis, orthomosaic analysis)	[141]
Different type of landslides	Displacement, Deformation, Change detection	Radar and optical satellites, UAVs, Ground radars, Laser scanners	InSAR (D-InSAR, PS-InSAR), GB-InSAR, Optical image analysis, 3D modeling analysis, LiDAR (DEM analysis), UAV photogrammetry (orthomosaic analysis)	[142]
Rock slides	Displacement, Deformation	Ground radars, Laser scanners, UAVs	GB-InSAR, TLS (3D modeling analysis), UAV photogrammetry (orthomosaic analysis)	[143]
Debris flows	Displacement	Optical satellites, UAVs	Optical images and orthomosaic analysis	[144]

4.6.1. Multidisciplinary Approaches

An advanced disaster warning system has been developed, using GNSS receivers, fracture meters, and rainfall gauges to monitor landslide precursors, i.e., displacements and deformations [133]. The system has been extended to monitor multi-temporal satellite imagery and use InSAR techniques. The analyses of landslide precursor events carried out on their basis, using available historical data, showed that displacements and deformations in the study area had already occurred decades before the event. Implementing RSTs for systematic monitoring of areas subject to pre-event observations could have predicted the occurrence of an event much earlier and avoided many economic losses.

Moreover, combining a network of geotechnical surface sensors (inclinometers) with InSAR data for landslide monitoring proved to be a solution for detecting slope failures on Gediminas Castle Hill [134]. The monitoring system, integrating the techniques above, enabled the observation of displacement on a large scale and over a period of time, detecting precursors of displacement before slope failures occur. The use of MT-InSAR with a wireless sensor network made of several bar extensometers and a borehole inclinometer to monitor landslides also helped to understand how rainfall can affect the rate of deformation and showed high agreement in the spatial and temporal distribution of deformation between the two monitoring techniques [139]. Thanks to their vast coverage, InSAR satellite data enable clear identification of spatial surface movements and their long-term evolution. Installed geotechnical sensors provide near-real-time information, which allows the identification of accelerations of rapid slope movements.

The selection of measurement techniques for monitoring landslides depends on the ground. A combination of multi-source remote sensing and Electrical Resistivity Tomog-

raphy (ERT) techniques for monitoring deformation and moisture changes is effective in loess areas. Integration of InSAR, TLS, and optical image interpretation has been used to monitor precursors of ground surface displacement over time [135]. The proposed system also overcame the difficulties encountered by InSAR technology in effectively capturing meter-long deformations using TLS. For permafrost areas, also requiring the selection of appropriate measurement techniques, precursors such as displacement, deformation, volume change, and landslide temperature have been studied [132]. The case of monitoring rock slide Vaslemanden (Norway) with several techniques shows (Table 3) how the complexity of structural conditions can hinder hazard management. Nevertheless, data from various sources enabled accurate monitoring of changes, which was crucial for disaster prevention and risk management.

Multidisciplinary approaches, including seismological records, the InSAR technique, and the analysis of optical satellite imagery, have been used to detect and locate unstable rock slopes [136]. Due to the lack of optical data in winter and problems with D-InSAR resolution on steep slopes, more than remote sensing data is needed for detailed analysis or prediction of rock slope failures. However, seismic, interferometric, and optical signatures of rock avalanche precursors provide early warning of potential new events. To better understand the kinematics and evolution of slope deformation, a monitoring system was developed using UAV-photogrammetry, PS-InSAR, GNSS reflectors, slope meters, and extensometers [137]. InSAR results confirmed by GNSS measurements showed displacement precursors. Extensometers and tiltmeters supported system performance by monitoring displacements and gaps. Data integration requires crucial analyses to establish alarm thresholds, but already at this stage, it enables comprehensive landslide monitoring.

The use of different measurement techniques, divided into mobile (measuring instruments are moved to collect data) and permanent (permanently installed and continuously collecting data) (Table 3), allowed the development of an innovative landslide monitoring system [138]. The proposed monitoring system was divided into three scales. The first is regional, using InSAR technology to detect and monitor landslides. The second, from regional to local scales, is based on UAVs and automated weather station measurements. The third is local, with an in situ visual monitoring camera system and groundwater level measurements. This system's main ideas include monitoring and detecting landslides on a regional scale and local monitoring of their behavior, which provides opportunities for innovative EWSs.

4.6.2. RS Approaches

The potential of several ground-based RSTs (Table 3) and their effectiveness in synergistic use have been investigated in several case studies analyzing different slope instability processes at various scales of emergency or post-disaster management [58]. The results confirmed that, for each of the analyzed cases, using a single monitoring technique may not be entirely sufficient due to inherent limitations, i.e., the range of detectable displacement velocity or the repeatability of data recording. By combining several RSTs, such as SAR, optical imagery, LiDAR, and IRT, an effective monitoring system for landslides and landslide activity can be established due to the diverse features of these instruments, thus overcoming the limitations of individual techniques.

Time series analysis based on the InSAR technique has the potential to provide essential knowledge on the precursors of large-scale landslide displacement and deformation. Unfortunately, this technique cannot fully capture rapid ground surface movements due to its limitations, i.e., low spatial and temporal resolution and phase noise. The proposed landslide monitoring solution integrates the SB-InSAR technique and UAV photogrammetry, providing high-resolution images and capturing the fastest surface movements [141]. However, the proposed combination of GB-SAR integrated with data acquired from satellites (e.g., Sentinel-1/2, TerraSAR-X, and SkyMED) has great potential to fully capture surface motions and improve the system. This can be confirmed by studies integrating InSAR and GB-InSAR techniques in geohazard monitoring [140,142]. The results showed that the

InSAR technique is effective in mapping unstable areas. However, as a standalone RST technique, it is only partially suitable for real-time landslide monitoring and early warning. With the additional use of GB-InSAR, characterized by high precision and frequency of measurements and the ability to take measurements in vegetated areas, the two techniques complement each other and form the basis of an effective monitoring system.

Attempts to overcome the problem arising from obtaining reliable results using InSAR in vegetated areas were made using the InSAR time series analysis technique using single and multi-view phases [50]. The main objective was to increase the number of measurement points in non-vegetated areas, which ultimately enabled the analysis of deformation's magnitude and dynamic evolution in different landslide parts. Additional studies based on optical imaging to determine landslide boundaries and UAV photogrammetry to create DTM and DEM for analyzing the landslide's characteristics confirmed the reliability of the results obtained using InSAR techniques. Based on the same RSTs, the possibility of predicting the failure time based on the analysis of deformation patterns before the event was demonstrated [20]. Thanks to the study's comprehensiveness, three different phases of mass movements (initiation, transport, and accumulation) were distinguished, providing essential information for improving landslide EWS and hazard assessment under similar geological and geomorphological conditions.

An integrated system based on GB-InSAR, TLS, and UAV photogrammetry enabled rapid analysis and evaluation of various aspects of small landslides, such as spatial distribution, volume, stability, potential expansion, extent of impact, and intensity [143]. GB-InSAR has been used to create displacement maps and velocity diagrams, making it possible to predict the kinematic evolution of a landslide. TLS contributed by rapidly modeling slopes and extracting geometric features of the landslide, which, when adjusted with GB-InSAR data, enabled the creation of a 3D deformation model, identifying potential landslide-prone areas. UAV photogrammetry was used to study hidden dangerous points and landslide-prone areas. Landslide deformation evolution and risk assessment of secondary landslide events were carried out using techniques from InSAR, GB-InSAR, and TLS [108]. Analyses of pre- and post-event displacements, stability of masses, and the activity status of long-term ground displacements were evaluated using PS-InSAR. This allowed the detection of potential precursors based on local time series accelerations. GB-InSAR enabled the monitoring of short-term sediment behavior after rockfall events. In addition, TLS data were used to create high-resolution 3D models that enabled displacement analysis over time by comparing successive measurement data sets. The integrated approaches in both cases overcame the limitations of individual techniques and enabled more comprehensive and accurate monitoring and analysis of landslides. Comprehensive data analysis, using integrations of GB-InSAR, TLS, and IRT techniques, additionally allowed for precursors of thermal anomalies [58]. Long-term monitoring, the creation of detailed 3D models, and the comparison of data enabled the detection of terrain changes. Thermal maps were crucial for identifying seepage sectors and rock mass discontinuities, allowing early detection of instability in areas with crack networks and block detachments.

An analysis of potential precursors was also carried out in a paper that presented a new approach to radar coherence analyses and the NDVI index to investigate the time series of landslide activity before failure [109]. Relatively easy-to-calculate radar coherence coefficients were determined on a large spatial scale to monitor unstable slopes. The results observed a decrease in radar coherence coefficient values, coinciding with the beginning of landslide acceleration, which was recorded several months before the failure. The advantage of the proposed approach is the elimination of the negative influence of long temporal baselines, which can interfere with the analysis of InSAR data, and interferences from atmospheric and vegetation cycles.

Using optical remote sensing data to develop a concept for quantitative evaluation of EWS landslide timing using UAV photogrammetry and satellite optical imagery (PlanetScope) was also a novel approach [144]. The digital image correlation (DIC) technique has been used to identify high-risk sites and to recognize landslide behavior by identifying

displacement precursors. Knowing the processing time of the data made it possible to estimate the time needed for warning actions, which is essential in creating EWSs.

5. Advantages and Limitations of Using RSTs to Analyze Landslide Precursors

RSTs have advantages and limitations (Table 4) that depend on their application. For the study of landslide precursors, the selection of appropriate techniques depends on the specifics and size of the area of interest, the type of landslide, and the pattern of deformation. This section discusses the advantages and limitations of using RSTs to analyze landslide precursors, as well as their effectiveness under different field conditions.

Table 4. Comparison of different RSTs with an overview of the advantages/limitations of the employed techniques with respect to landslides and precursor types.

RST	Sensors for Monitoring	Landslide Type	Advantages	Limitations			
SAR	Satellites with radar sensors		<ul style="list-style-type: none">large-scale and long-time series of surface deformation [21,83]detection of early deformed slopes and prediction of potential failure slopes [83]availability of historical data [21]day and night data acquisition and all weather conditions [145]	<ul style="list-style-type: none">identification of loss of coherence, i.e., phase decorrelation [26]detection of fast movement [28]overcoming the limitations of InSAR in regions with low coherence [30]millimeter accuracy (MT-InSAR) [147]atmospheric effects correction using MT-InSAR techniques [83]ability to detect slow landslides [147]	<ul style="list-style-type: none">low spatial, volume, and temporal resolution [22,146]the phase gradient data limit the magnitude and extent of capture deformation characteristics [83]spatial decorrelation for such land types as high vegetation cover, water areas, and surface roughness [30,83]phase ambiguity [51]phase noise caused by differential phase generated by DEM errors and orbital inaccuracies [51]postponed time [21]	<ul style="list-style-type: none">lack of ability to determine numerical displacement values [110]monitoring decimeter displacements [31]atmospheric phase delay (D-InSAR) [21]	
		CCD					
		OT		<ul style="list-style-type: none">translational and rotational slidesrock slidesdeep-seated landslidescreeping landslides and flowslateral spread			
		InSAR					
GB-InSAR	Ground-based radars	<ul style="list-style-type: none">translational slidesrockfallsrock slidesslow and moderate-type landslidescomplex landslideslateral spread	<ul style="list-style-type: none">high spatial and temporal resolution [145]long term monitoring [21]early warning and rapid assessment of risk scenarios [21]day and night data acquisition [125]measuring steep slopes [67]	<ul style="list-style-type: none">coherence, temporal and spatial decorrelation due to vegetation cover [71,145]atmospheric conditions, such as rain, fog, or atmospheric turbulence, introduce noise and errors into the data [76,78,148]displacement along the line of sight [125,149]limited observation radius [69]			

Table 4. Cont.

RST	Sensors for Monitoring	Landslide Type	Advantages		Limitations	
Optical images	Satellites, UAVs with digital cameras	<ul style="list-style-type: none"> shallow soil landslides 	<ul style="list-style-type: none"> superior capture accuracy with high spatial, temporal, and spectral resolution optical images [83] continuous characteristics of time series evolution with medium-resolution optical images [83] approach to delineate landslide-affected areas [21] multiple platforms [21] low cost [125] 		<ul style="list-style-type: none"> bias and blur in spectral imaging [83] acquisition limited to daylight [21] weather and cloud cover dependence [14,47] establishment of landslide boundaries [20] accuracy of photo interpretation is slightly low [87] changing land coverage [127] areas covered with dense vegetation [39] 	
Multispectral (MS)/Hyperspectral images	Satellites/UAVs with multispectral/hyperspectral sensors	<ul style="list-style-type: none"> translational slides deep seated landslides creeping landslides and flows slow and moderate-type landslides complex landslides shallow soil landslides 	<ul style="list-style-type: none"> enhanced spectral information, allowing for the extraction of valuable information about various land surface properties related to landslide precursors [109] detecting changes over time [125] wide area coverage [14] 		<ul style="list-style-type: none"> acquisition limited to daylight [21] weather and cloud cover dependence [35] 	
LiDAR	TLS	<ul style="list-style-type: none"> rockfalls rock slides slow-moving landslides 	<ul style="list-style-type: none"> high-resolution data [87] ability to penetrate vegetation [2] high-resolution terrain models [145] 	<ul style="list-style-type: none"> 3D capabilities [145] 	<ul style="list-style-type: none"> point cloud resolution related to scene distance [21] data acquisition dependent on weather [145] high equipment cost [87] 	<ul style="list-style-type: none"> ground control points needed for high-quality 3D product results [35]
	ALS	<ul style="list-style-type: none"> debris flows earth flows mud flows lateral spread 	<ul style="list-style-type: none"> detection of unstable masses by calculating volumes [21] 	<ul style="list-style-type: none"> rapid acquisition of large data sets, enabling efficient monitoring of wide regions [145] 		<ul style="list-style-type: none"> less accuracy compared with TLS [145] low temporal resolution [35]

Table 4. Cont.

RST	Sensors for Monitoring	Landslide Type	Advantages	Limitations
IRT	Satellites/UAVs with thermographic cameras	<ul style="list-style-type: none">cracks and fractures within rock slopes	<ul style="list-style-type: none">high-resolution data [145]day and night data acquisition [21,150]sustained increases in trends and peaks in temperature provide the initiation time of landslides [83]large range and long time series of surface temperature data [83]	<ul style="list-style-type: none">restricted to low-temperature use [145]thermal differences related to slope orientation, surface roughness, and solar radiation [21]

SAR offers significant advantages, enabling the search and analysis of detected landslide precursors. The most important of these include the ability to cover vast areas that may be inaccessible for measurement by classical techniques. The weather-independent SAR technique allows penetration through fog, clouds, and light rain [145]. These techniques use long time series to estimate and remove the atmospheric component of the interferometric phase [83]. In addition to studying the evolution of landslides over time, including historical analysis [21], these techniques can provide time series and maps of mean ground surface displacements [38]. Combining techniques that detect slower [147] and fast movements [28] allows the techniques to complement each other, resulting in the ability to monitor landslides with different displacement rates. The phase-based (e.g., PS-InSAR) approach can detect movements of several tens of cm per year, while the minimum detectable values for the amplitude-based (e.g., OT) approach are a few meters [151]. The difficulties encountered in determining the total deformation range have been resolved using the two-phase MT-InSAR technique, which allows precise monitoring of movements with different displacement scales [37].

In contrast to data acquired from satellite platforms, GB-InSAR can provide images with high spatial [74] and temporal resolution [145]. It enables monitoring landslides in hard-to-reach areas without needing to install sensors in the study area [78]. Moreover, contrary to satellite images, GB-InSAR can operate on steep slopes [67].

Technological advances and access to open-source optical data (e.g., from Sentinel-2) allow for continuous characterization of the evolution of the displacement time series despite the medium resolution of the delivered products [83]. Developing various data processing algorithms based on high-resolution optical images enables the determination of ground surface displacements of single-centimeter values [35]. Multispectral and hyperspectral data can provide important precursors to landslides by allowing the extraction of valuable information from calculated vegetation indices, such as changes in vegetation conditions or moisture in landslide areas [109].

LiDAR techniques, on the other hand, have the ability to penetrate vegetation, facilitating the monitoring of vegetated areas [2]. Considering the ability to accurately monitor slope deformation, TLS is characterized by high accuracy, spatial resolution, and the ability to create high-resolution terrain models [87]. With its ability to rapidly acquire large datasets, ALS enables efficient monitoring on a larger scale [152]. Both of the techniques offer the possibility of detecting changes in the ground surface by, among other things, calculating volumes [21].

The advantage of the IRT technique is that it provides information on the timing of landslide initiation based on sustained trends in temperature rise and peak values [83]. The technique provides high-resolution data [145] and the ability to acquire data regardless of the time of day [150] and visibility [153].

Despite the development of SAR techniques over the decades, monitoring landslides covered by vegetation remains a challenge due to low temporal resolution [22], especially for L-band satellite data, which plays a significant role during landslide investigations due to L-band's ability to penetrate vegetation [146]. The solution could be to use data acquired from the L-band-equipped NISAR satellite and integrate C-band and L-band images, enabling deeper vegetation penetration with higher spatial resolution [154]. Unfortunately, this satellite is still waiting to be launched into space. In addition, phase ambiguity, phase noise, atmospheric phase delay, topographic errors, and spatial decorrelation significantly impact the results [30,151]. Although several studies have taken steps to develop a procedure for correcting phase unwrapping errors and tropospheric delay correction, this problem remains an obstacle, resulting in errors in the determined displacements of up to several tens of centimeters [155]. D-InSAR also encounters some difficulties related to, among other things, loss of integrity due to dense vegetation cover [30]. Additionally, the technique allows the detection of displacements with centimeter accuracy in the line of sight (LOS) [156]. When detecting deep-seated landslides moving at a rate of a few millimeters per year, the technique may not yield the expected results.

Similar to SAR, the GB-InSAR technique also encounters limitations, such as phase wrapping, noise effects, and spatial and temporal decorrelation, due to dense vegetation in the monitored area [71], terrain topography, and weather conditions [78,148]. In addition, the system can only measure the motion component parallel to the LOS [125,149]. This leads to the omission of displacements occurring in the direction perpendicular to the sensor [71,149]. The search for novel solutions may allow the gap in real-time data processing to be closed through the use of appropriate filters, i.e., the Kalman filter [76].

Optical, multispectral, and hyperspectral images face limitations related to the ability to obtain data only in daylight [21] and dependence on weather and cloud cover conditions [14,47]. In addition, the changing land coverage [127] and dense vegetation of the monitored areas [39] make it difficult to interpret the acquired data or may lead to errors in the obtained results.

Limitations of using TLS to analyze landslide precursors include difficulties penetrating the forest or measuring in hard-to-reach areas, such as mountainous areas, and the need to use ground control points to obtain high-quality products [35]. However, ALS may encounter difficulties with measurement accuracy in areas with high topographical variability and require significant financial and logistical resources [87]. In addition, both techniques are susceptible to atmospheric conditions, which can limit their effectiveness in some situations and reduce the amount of data acquired [152].

Atmospheric conditions, such as clouds, humidity, or low temperatures, can affect the precision of IRT measurements, making the results difficult to interpret [145]. Variable terrain topography also negatively affects the interpretation of thermal imaging data [21].

6. Discussion

The effectiveness of EWSs based entirely on RSTs has yet to be completely investigated. Attempts to quantify the lead time of landslide EWS, analyzing the time to issue an alert, which consisted of the time to collect, process, and evaluate data using UAV photogrammetry and satellite optical images, allowed landslides to be predicted up to several hours in advance [144]. However, integrating additional RSTs and using advanced data processing algorithms can reduce this time. Such systems should consider the risk of false alarms that can occur due to misinterpretation of data in areas whose structure has changed (human activity, vegetation growth) and errors caused by various data disturbances. Scenarios for solving such problems should be developed to minimize their occurrence in the future. They should include such measures as regular calibration of equipment (optical, multispectral, and hyperspectral cameras, scanners, and radars), advanced algorithms to reduce noise and measurement errors, and data validation (using permanent GNSS stations). Unlike false alarms, undetected events can lead to more severe consequences, such as human and material losses. They can be caused by delayed response times due to the need to process large amounts of data, occurring noise and disturbance, and their low spatial and temporal resolution, leading to the omission of important details. Developing an automated system with advanced algorithms and integrating RST data will enable faster data processing and a complete view of changes detected by different techniques, ultimately eliminating these problems.

Implementing remote sensing-based EWSs, especially on a large scale, involves costs due to the need to acquire equipment, i.e., ground-based radars, laser scanners, thermal, optical, and multispectral cameras, and their maintenance and servicing. Monitoring particular areas or slow-moving landslides requires high-resolution satellite data that can be obtained from commercial sources, which entails an additional investment. In addition, providing a robust infrastructure to store, process, and deliver massive amounts of data requires servers, efficient computers, and appropriate software. In order to maintain the reliability and accuracy of results, regular updates to software, systems, and databases, improving algorithms, updating data, and optimizing performance are crucial. Implementing standardized data collection, processing, and analysis procedures is crucial to ensuring consistency in data analysis and avoiding errors due to inconsistent research and

interpretation methods. An essential element of remote sensing-based EWSs is the prompt delivery of results to relevant parties for effective warning of impending threats. Therefore, it is necessary to develop notification and alert systems, i.e., web-based platforms, mobile applications, or regular reporting showing threats and future forecasts.

For EWSs to effectively and efficiently counter hazards, they need to actively engage stakeholders and end-users to report any problems that arise in the systems and promptly initiate evacuation actions. In areas that require detailed investigations or are at risk, analysis of historical data and consultation with local experts are required, which can extend the decision-making process. Even advanced technological monitoring systems are only effective if they reach the population in time and evacuation measures are taken. Therefore, raising risk awareness among the population is crucial, reducing the probability of hazardous behavior and increasing the effectiveness of landslide warnings.

In the rapidly evolving technological environment, measurement and data analysis techniques based on artificial intelligence (AI), i.e., machine learning (ML) and deep learning (DL), have found applications in detecting changes formed on the land surface, especially shallow landslides [86]. It has improved landslide monitoring systems, enabling the automation of computational processes and accelerated data analysis, mainly of radar and optical images. Future directions for improving existing EWSs include these innovations and improving RSTs and their integration. One example attempts to develop a prototype drone-borne radar that significantly improves the temporal resolution of SAR techniques [157]. With this approach, it will be possible to rapidly respond to sudden events (rainfall, earthquakes) that occur locally, especially in hard-to-reach areas, i.e., mountainous and forested areas. ML and DL techniques allow automatic analysis of vast amounts of data, detection of patterns and trends in data, and prediction of phenomena based on previous observations [158,159]. Using them can improve the identification of landslide precursors and allow for more accurate predictions of future events, thereby improving the performance of existing EWS and expanding them to a regional scale [160,161]. Convolutional neural networks (CNNs) effectively extract features from images, making it possible to automatically predict landslides on a regional scale by crowdsourcing optical images [162]. The DIC technique enables the determination of displacements over large areas [85,99]. Using high-resolution ground-based optical images enables continuous measurement of active landslides with displacements amounting to one m/day [163]. Also, the use of several new modern approaches in photogrammetry, such as structure from motion (SfM), Object-Based Image Analysis (OBIA), and simultaneous localization and mapping (SLAM), can support EWSs [164,165]. Despite increasingly innovative solutions, further research is needed to overcome limitations, such as limited spatial and temporal coverage, selection of suitable RSTs, the complexity of data processing, dense vegetation, atmospheric phase delay, topographic error, large workload, interpretation, and validation challenges (Table 4).

7. Summary

This article reviews 165 articles on detecting, monitoring, predicting, and identifying landslide precursors using RSTs. The application and integration of RSTs and their advantages and limitations in detecting landslide precursors were also analyzed. It was noted that the integration of RSTs should be selected not only based on the type of area monitored, the type of landslides, or their deformation patterns but also considering the appropriate temporal and spatial resolution of data acquisition, the expected results (metric values or visual changes), or their measurement accuracy. It was found that creating the best possible system for detecting landslide precursors on a regional scale should integrate techniques that provide high-resolution, weather- and illumination-independent (SAR) data, offer a broad perspective and regularity for monitoring large areas (optical and multispectral/hyperspectral images, IRT), and provide precise, detailed, and timely data for high-risk areas and complex terrain (LiDAR, GB-InSAR). This combination can provide a more complete and accurate view of changes and continuous, reliable system operation, even during temporary interruptions or disruptions in any of the techniques.

The integration of RSTs with advanced algorithms that optimize computational processes and data analysis is expected to accelerate the identification of landslide precursors in existing EWSs and enable their detection on a regional scale. In addition, the difficulty of monitoring, especially in mountainous areas with permafrost, dense vegetation, and steep slopes, will be a priority for the future development of RSTs. Monitoring deep-seated, slow-moving landslides, which can have annual displacements of several mm per year, also poses additional challenges, underscoring the need for further research to optimize and adapt measurement techniques to specific regional conditions and landslide types.

Despite all these difficulties, it is vital to consider the social aspects. No matter how technologically advanced monitoring and EWSs based on RSTs are developed, their effectiveness is limited if they do not reach the population in time and no evacuation measures are taken [2]. Therefore, in addition to the scientific aspect, it is crucial to raise awareness of the risks among the population, which will undoubtedly reduce the likelihood of dangerous behaviors and increase the effectiveness of landslide warnings.

Author Contributions: Conceptualization, K.S. and P.Ć.; methodology, K.S. and E.P.; investigation, K.S.; writing—original draft preparation, K.S.; writing—review and editing, P.Ć. and E.P.; visualization, K.S.; supervision, P.Ć. and E.P.; project administration, P.Ć.; funding acquisition, P.Ć. All authors have read and agreed to the published version of the manuscript.

Funding: This research project was supported by the program “Excellence Initiative—Research University” at the AGH University of Krakow.

Conflicts of Interest: The authors declare no conflicts of interest.

References

1. Wu, Q.; Qin, Y.; Tang, H.; Meng, Z.; Li, C.; Lu, S. Influence of Wetting and Drying Cycles on the Shear Behavior of Discontinuities between Two Different Rock Types with Various Surface Topographies. *Acta Geotech.* **2024**. [\[CrossRef\]](#)
2. Casagli, N.; Intrieri, E.; Tofani, V.; Gigli, G.; Raspini, F. Landslide Detection, Monitoring and Prediction with Remote-Sensing Techniques. *Nat. Rev. Earth Environ.* **2023**, *4*, 51–64. [\[CrossRef\]](#)
3. Liu, S.; Segoni, S.; Raspini, F.; Yin, K.; Zhou, C.; Zhang, Y.; Casagli, N. Satellite InSAR as a New Tool for the Verification of Landslide Engineering Remedial Works at the Regional Scale: A Case Study in the Three Gorges Reservoir Area, China. *Appl. Sci.* **2020**, *10*, 6435. [\[CrossRef\]](#)
4. Prestininzi, A.; Bianchi-Fasani, G.; Bozzano, F.; Esposito, C.; Martino, S.; Mazzanti, P.; Scarascia-Mugnozza, G. From the Refinement of Geological Models to Risk Management: The Role of Landslide Monitoring. In *Landslides and Engineered Slopes: Protecting Society through Improved Understanding*; Taylor & Francis Group: London, UK, 2012.
5. Pecoraro, G.; Calvello, M.; Piciullo, L. Monitoring Strategies for Local Landslide Early Warning Systems. *Landslides* **2019**, *16*, 213–231. [\[CrossRef\]](#)
6. Gian, Q.A.; Tran, D.-T.; Nguyen, D.C.; Nhu, V.H.; Tien Bui, D. Design and Implementation of Site-Specific Rainfall-Induced Landslide Early Warning and Monitoring System: A Case Study at Nam Dan Landslide (Vietnam). *Geomat. Nat. Hazards Risk* **2017**, *8*, 1978–1996. [\[CrossRef\]](#)
7. Auflīč, M.J.; Herrera, G.; Mateos, R.M.; Poyiadji, E.; Quental, L.; Severine, B.; Peternel, T.; Podolszki, L.; Calcaterra, S.; Kociu, A.; et al. Landslide Monitoring Techniques in the Geological Surveys of Europe. *Landslides* **2023**, *20*, 951–965. [\[CrossRef\]](#)
8. Jemec Auflīč, M.; Komac, M.; Šinigoj, J. Modern Remote Sensing Techniques for Monitoring Pipeline Displacements in Relation to Landslides and Other Slope Mass Movements. In *Environmental Security of the European Cross-Border Energy Supply Infrastructure*; Culshaw, M.G., Osipov, V.I., Booth, S.J., Victorov, A.S., Eds.; NATO Science for Peace and Security Series C: Environmental Security; Springer: Dordrecht, The Netherlands, 2015; ISBN 978-94-017-9537-1. [\[CrossRef\]](#)
9. Michoud, C.; Bazin, S.; Blikra, L.H.; Derron, M.-H.; Jaboyedoff, M. Experiences from Site-Specific Landslide Early Warning Systems. *Nat. Hazards Earth Syst. Sci.* **2013**, *13*, 2659–2673. [\[CrossRef\]](#)
10. Brunetti, M.T.; Melillo, M.; Gariano, S.L.; Ciabatta, L.; Brocca, L.; Amarnath, G.; Peruccacci, S. Satellite Rainfall Products Outperform Ground Observations for Landslide Prediction in India. *Hydrol. Earth Syst. Sci.* **2021**, *25*, 3267–3279. [\[CrossRef\]](#)
11. Liu, G.; Guo, H.; Perski, Z.; Fan, J.; João Sousa, J.; Yan, S.; Tang, P. Landslide Movement Monitoring with ALOS-2 SAR Data. *IOP Conf. Ser. Earth Environ. Sci.* **2019**, *227*, 062015. [\[CrossRef\]](#)
12. Carlà, T.; Intrieri, E.; Farina, P.; Casagli, N. A New Approach to Assess the Stability of Rock Slopes and Identify Impending Failure Conditions. In *Advancing Culture of Living with Landslides*; Mikos, M., Tiwari, B., Yin, Y., Sassa, K., Eds.; Springer International Publishing: Cham, Switzerland, 2017; pp. 733–739, ISBN 978-3-319-53497-8.
13. Intrieri, E.; Raspini, F.; Fumagalli, A.; Lu, P.; Del Conte, S.; Farina, P.; Allievi, J.; Ferretti, A.; Casagli, N. The Maoxian Landslide as Seen from Space: Detecting Precursors of Failure with Sentinel-1 Data. *Landslides* **2018**, *15*, 123–133. [\[CrossRef\]](#)

14. Lacroix, P.; Bièvre, G.; Pathier, E.; Kniess, U.; Jongmans, D. Use of Sentinel-2 Images for the Detection of Precursory Motions before Landslide Failures. *Remote Sens. Environ.* **2018**, *215*, 507–516. [\[CrossRef\]](#)
15. Martín-Martín, A.; Thelwall, M.; Orduna-Malea, E.; Delgado López-Cózar, E. Google Scholar, Microsoft Academic, Scopus, Dimensions, Web of Science, and OpenCitations' COCI: A Multidisciplinary Comparison of Coverage via Citations. *Scientometrics* **2021**, *126*, 871–906. [\[CrossRef\]](#) [\[PubMed\]](#)
16. Martín-Martín, A.; Orduna-Malea, E.; Thelwall, M.; Delgado López-Cózar, E. Google Scholar, Web of Science, and Scopus: A Systematic Comparison of Citations in 252 Subject Categories. *J. Informetr.* **2018**, *12*, 1160–1177. [\[CrossRef\]](#)
17. Orduna-Malea, E.; Martín-Martín, A.; Delgado López-Cózar, E. Google Scholar Como Una Fuente de Evaluación Científica: Una Revisión Bibliográfica Sobre Errores de La Base de Datos. *Rev. Esp. Doc. Científica* **2017**, *40*, 185. [\[CrossRef\]](#)
18. Singh, V.K.; Singh, P.; Karmakar, M.; Leta, J.; Mayr, P. The Journal Coverage of Web of Science, Scopus and Dimensions: A Comparative Analysis. *Scientometrics* **2021**, *126*, 5113–5142. [\[CrossRef\]](#)
19. Moher, D.; Liberati, A.; Tetzlaff, J.; Altman, D.G. The PRISMA Group Preferred Reporting Items for Systematic Reviews and Meta-Analyses: The PRISMA Statement. *PLoS Med.* **2009**, *6*, e1000097. [\[CrossRef\]](#) [\[PubMed\]](#)
20. Yi, Z.; Xingmin, M.; Allesandro, N.; Tom, D.; Guan, C.; Colm, J.; Yuanxi, L.; Xiaojun, S. Characterization of Pre-Failure Deformation and Evolution of a Large Earthflow Using InSAR Monitoring and Optical Image Interpretation. *Landslides* **2022**, *19*, 35–50. [\[CrossRef\]](#)
21. Casagli, N.; Frodella, W.; Morelli, S.; Tofani, V.; Ciampalini, A.; Intrieri, E.; Raspini, F.; Rossi, G.; Tanteri, L.; Lu, P. Spaceborne, UAV and Ground-Based Remote Sensing Techniques for Landslide Mapping, Monitoring and Early Warning. *Geoenviron. Disasters* **2017**, *4*, 9. [\[CrossRef\]](#)
22. Zhao, C.; Lu, Z.; Zhang, Q.; de la Fuente, J. Large-Area Landslide Detection and Monitoring with ALOS/PALSAR Imagery Data over Northern California and Southern Oregon, USA. *Remote Sens. Environ.* **2012**, *124*, 348–359. [\[CrossRef\]](#)
23. Yao, X.; Chen, Y.; Liu, D.; Zhou, Z.; Liesenberg, V.; Marcato Junior, J.; Li, J. Average-DInSAR Method for Unstable Escarpments Detection Induced by Underground Coal Mining. *Int. J. Appl. Earth Obs. Geoinf.* **2021**, *103*, 102489. [\[CrossRef\]](#)
24. Liu, Y.; Liao, M.; Shi, X.; Zhang, L.; Cunningham, C. Potential Loess Landslide Deformation Monitoring Using L-Band SAR Interferometry. *Geo-Spat. Inf. Sci.* **2016**, *19*, 273–277. [\[CrossRef\]](#)
25. Yin, H.Y.; Lee, C.Y.; Lin, C.W.; Chen, R.F.; Chang, C.S.; Chi, C.Y. A Nationwide Catastrophic Landslide Hazard Assessment in Taiwan. In Proceedings of the 17th European Conference on Soil Mechanics and Geotechnical Engineering (ECSMGE), Reykjavik, Iceland, 1–6 September 2019; International Society for Soil Mechanics and Geotechnical Engineering: London, UK, 2019; pp. 2549–2555. [\[CrossRef\]](#)
26. Tzouvaras, M.; Danezis, C.; Hadjimitsis, D.G. Small Scale Landslide Detection Using Sentinel-1 Interferometric SAR Coherence. *Remote Sens.* **2020**, *12*, 1560. [\[CrossRef\]](#)
27. Smail, T.; Abed, M.; Mebarki, A.; Lazecky, M. Earthquake-Induced Landslide Monitoring and Survey by Means of InSAR. *Nat. Hazards Earth Syst. Sci.* **2022**, *22*, 1609–1625. [\[CrossRef\]](#)
28. Solari, L.; Raspini, F.; Del Soldato, M.; Bianchini, S.; Ciampalini, A.; Ferrigno, F.; Tucci, S.; Casagli, N. Satellite Radar Data for Back-Analyzing a Landslide Event: The Ponzano (Central Italy) Case Study. *Landslides* **2018**, *15*, 773–782. [\[CrossRef\]](#)
29. Yin, Y.; Liu, X.; Zhao, C.; Tomás, R.; Zhang, Q.; Lu, Z.; Li, B. Multi-Dimensional and Long-Term Time Series Monitoring and Early Warning of Landslide Hazard with Improved Cross-Platform SAR Offset Tracking Method. *Sci. China Technol. Sci.* **2022**, *65*, 1891–1912. [\[CrossRef\]](#)
30. Qu, T.; Lu, P.; Liu, C.; Wu, H.; Shao, X.; Wan, H.; Li, N.; Li, R. Hybrid-SAR Technique: Joint Analysis Using Phase-Based and Amplitude-Based Methods for the Xishancun Giant Landslide Monitoring. *Remote Sens.* **2016**, *8*, 874. [\[CrossRef\]](#)
31. Zhu, Y.; Qiu, H.; Liu, Z.; Wang, J.; Yang, D.; Pei, Y.; Ma, S.; Du, C.; Sun, H.; Wang, L. Detecting Long-Term Deformation of a Loess Landslide from the Phase and Amplitude of Satellite SAR Images: A Retrospective Analysis for the Closure of a Tunnel Event. *Remote Sens.* **2021**, *13*, 4841. [\[CrossRef\]](#)
32. Jia, H.; Zhang, H.; Liu, L.; Liu, G. Landslide Deformation Monitoring by Adaptive Distributed Scatterer Interferometric Synthetic Aperture Radar. *Remote Sens.* **2019**, *11*, 2273. [\[CrossRef\]](#)
33. Wang, C.; Li, Q.; Zhu, J.; Gao, W.; Shan, X.; Song, J.; Ding, X. Formation of the 2015 Shenzhen Landslide as Observed by SAR Shape-from-Shading. *Sci. Rep.* **2017**, *7*, 43351. [\[CrossRef\]](#)
34. Manconi, A.; Kourkoulis, P.; Caduff, R.; Strozzi, T.; Loew, S. Monitoring Surface Deformation over a Failing Rock Slope with the ESA Sentinels: Insights from Moosfluh Instability, Swiss Alps. *Remote Sens.* **2018**, *10*, 672. [\[CrossRef\]](#)
35. Wasowski, J.; Bovenga, F. Remote Sensing of Landslide Motion with Emphasis on Satellite Multitemporal Interferometry Applications. In *Landslide Hazards, Risks, and Disasters*; Elsevier: Amsterdam, The Netherlands, 2015; pp. 345–403, ISBN 978-0-12-396452-6.
36. Lazecký, M.; Hatton, E.; González, P.J.; Hlaváčová, I.; Jiráňková, E.; Dvořák, F.; Šustr, Z.; Martinovič, J. Displacements Monitoring over Czechia by IT4S1 System for Automatised Interferometric Measurements Using Sentinel-1 Data. *Remote Sens.* **2020**, *12*, 2960. [\[CrossRef\]](#)
37. Zhang, B.; Wang, Y. An Improved Two-Step Multitemporal SAR Interferometry Method for Precursory Slope Deformation Detection Over Nanyu Landslide. *IEEE Geosci. Remote Sens. Lett.* **2021**, *18*, 592–596. [\[CrossRef\]](#)

38. Bovenga, F.; Argentiero, I.; Refice, A.; Nutricato, R.; Nitti, D.O.; Pasquariello, G.; Spilotro, G. Assessing the Potential of Long, Multi-Temporal SAR Interferometry Time Series for Slope Instability Monitoring: Two Case Studies in Southern Italy. *Remote Sens.* **2022**, *14*, 1677. [\[CrossRef\]](#)
39. Ouyang, C.; Zhao, W.; An, H.; Zhou, S.; Wang, D.; Xu, Q.; Li, W.; Peng, D. Early Identification and Dynamic Processes of Ridge-Top Rockslides: Implications from the Su Village Landslide in Suichang County, Zhejiang Province, China. *Landslides* **2019**, *16*, 799–813. [\[CrossRef\]](#)
40. Yao, J.; Yao, X.; Liu, X. Landslide Detection and Mapping Based on SBAS-InSAR and PS-InSAR: A Case Study in Gongjue County, Tibet, China. *Remote Sens.* **2022**, *14*, 4728. [\[CrossRef\]](#)
41. Shankar, H.; Singh, D.; Chauhan, P. Landslide Deformation and Temporal Prediction of Slope Failure in Himalayan Terrain Using PSInSAR and Sentinel-1 Data. *Adv. Space Res.* **2022**, *70*, 3917–3931. [\[CrossRef\]](#)
42. Raspini, F.; Bianchini, S.; Ciampalini, A.; Del Soldato, M.; Montalti, R.; Solari, L.; Tofani, V.; Casagli, N. Persistent Scatterers Continuous Streaming for Landslide Monitoring and Mapping: The Case of the Tuscany Region (Italy). *Landslides* **2019**, *16*, 2033–2044. [\[CrossRef\]](#)
43. Poyraz, F.; Gül, Y.; Duymaz, B. Determination of Deformations by Using the PSI Technique at a Common Dump Site of Three Different Open-Pit Marble Mines in Turkey. *Turk. J. Earth Sci.* **2020**, *29*, 1004–1016. [\[CrossRef\]](#)
44. Dun, J.; Feng, W.; Yi, X.; Zhang, G. Monitoring the Two-Dimensional Deformation of the Old Landslide in Woda Village with Radar Interferometry Technology. *IOP Conf. Ser. Earth Environ. Sci.* **2021**, *861*, 072030. [\[CrossRef\]](#)
45. Kuri, M.; Arora, M.K.; Bhattacharya, A.; Sharma, M.L. Microwave Remote Sensing Based Small Baseline Subset Technique for Estimation of Slope Movement in Nainital Area, India. In Proceedings of the 2017 Fourth International Conference on Image Information Processing (ICIIP), Shimla, India, 21–23 December 2017; IEEE: New York, NY, USA, 2017; pp. 1–6.
46. Zhao, C.; Zhang, Q.; He, Y.; Peng, J.; Yang, C.; Kang, Y. Small-Scale Loess Landslide Monitoring with Small Baseline Subsets Interferometric Synthetic Aperture Radar Technique—Case Study of Xingyuan Landslide, Shaanxi, China. *J. Appl. Remote Sens.* **2016**, *10*, 026030. [\[CrossRef\]](#)
47. Sepúlveda, S.A.; Alfaro, A.; Lara, M.; Carrasco, J.; Olea-Encina, P.; Rebolledo, S.; Garcés, M. An Active Large Rock Slide in the Andean Paraglacial Environment: The Yerba Loca Landslide, Central Chile. *Landslides* **2021**, *18*, 697–705. [\[CrossRef\]](#)
48. Huang, C.; Zhou, Q.; Zhou, L.; Cao, Y. Ancient Landslide in Wanzhou District Analysis from 2015 to 2018 Based on ALOS-2 Data by QPS-InSAR. *Nat. Hazards* **2021**, *109*, 1777–1800. [\[CrossRef\]](#)
49. Zhang, L.; Ding, X.; Lu, Z. Ground Settlement Monitoring Based on Temporarily Coherent Points between Two SAR Acquisitions. *ISPRS J. Photogramm. Remote Sens.* **2011**, *66*, 146–152. [\[CrossRef\]](#)
50. Liu, Z.; Qiu, H.; Zhu, Y.; Liu, Y.; Yang, D.; Ma, S.; Zhang, J.; Wang, Y.; Wang, L.; Tang, B. Efficient Identification and Monitoring of Landslides by Time-Series InSAR Combining Single- and Multi-Look Phases. *Remote Sens.* **2022**, *14*, 1026. [\[CrossRef\]](#)
51. Ciuffi, P.; Bayer, B.; Berti, M.; Franceschini, S.; Simoni, A. Deformation Detection in Cyclic Landslides Prior to Their Reactivation Using Two-Pass Satellite Interferometry. *Appl. Sci.* **2021**, *11*, 3156. [\[CrossRef\]](#)
52. Lindsay, E.; Frauenfelder, R.; Rüther, D.; Nava, L.; Rubensdotter, L.; Strout, J.; Nordan, S. Multi-Temporal Satellite Image Composites in Google Earth Engine for Improved Landslide Visibility: A Case Study of a Glacial Landscape. *Remote Sens.* **2022**, *14*, 2301. [\[CrossRef\]](#)
53. Sivasankar, T.; Ghosh, S.; Joshi, M. Exploitation of Optical and SAR Amplitude Imagery for Landslide Identification: A Case Study from Sikkim, Northeast India. *Environ. Monit. Assess.* **2021**, *193*, 386. [\[CrossRef\]](#)
54. Wang, C.; Shan, W.; Guo, Y.; Hu, Z.; Jiang, H. Relative Factors of Beihei Highway's Ground Deformation Interpretation Based on Remote-Sensing Imagery Technology. In *Landslides in Cold Regions in the Context of Climate Change*; Environmental Science and Engineering; Springer International Publishing: Cham, Switzerland, 2014; pp. 191–204, ISBN 978-3-319-00866-0.
55. Ramirez, R.; Abdullah, R.E.; Jang, W.; Choi, S.-K.; Kwon, T.-H. Satellite-Based Monitoring of an Open-Pit Mining Site Using Sentinel-1 Advanced Radar Interferometry: A Case Study of the December 21, 2020, Landslide in Toledo City, Philippines. *E3S Web Conf.* **2023**, *415*, 05020. [\[CrossRef\]](#)
56. Hanssen, R.F. *Radar Interferometry: Data Interpretation and Error Analysis*; Remote Sensing and Digital Image Processing; Springer: Dordrecht, The Netherlands, 2001; Volume 2, ISBN 978-0-7923-6945-5.
57. Crosetto, M.; Monserrat, O.; Cuevas-González, M.; Devanthéry, N.; Crippa, B. Persistent Scatterer Interferometry: A Review. *ISPRS J. Photogramm. Remote Sens.* **2016**, *115*, 78–89. [\[CrossRef\]](#)
58. Casagli, N.; Morelli, S.; Frodella, W.; Intrieri, E.; Tofani, V. TXT-Tool 2.039-3.2 Ground-Based Remote Sensing Techniques for Landslides Mapping, Monitoring and Early Warning. In *Landslide Dynamics: ISDR-ICL Landslide Interactive Teaching Tools*; Sassa, K., Guzzetti, F., Yamagishi, H., Arbanas, Ž., Casagli, N., McSaveney, M., Dang, K., Eds.; Springer International Publishing: Cham, Switzerland, 2018; pp. 255–274, ISBN 978-3-319-57773-9.
59. Liu, Z.; Xu, B.; Wang, Q.; Yu, W.; Miao, Z. Monitoring Landslide Associated with Reservoir Impoundment Using Synthetic Aperture Radar Interferometry: A Case Study of the Yalong Reservoir. *Geod. Geodyn.* **2022**, *13*, 138–150. [\[CrossRef\]](#)
60. Solari, L.; Barra, A.; Herrera, G.; Bianchini, S.; Monserrat, O.; Béjar-Pizarro, M.; Crosetto, M.; Sarro, R.; Moretti, S. Fast Detection of Ground Motions on Vulnerable Elements Using Sentinel-1 InSAR Data. *Geomat. Nat. Hazards Risk* **2018**, *9*, 152–174. [\[CrossRef\]](#)
61. Berti, M.; Corsini, A.; Franceschini, S.; Iannacone, J.P. Automated Classification of Persistent Scatterers Interferometry Time Series. *Nat. Hazards Earth Syst. Sci.* **2013**, *13*, 1945–1958. [\[CrossRef\]](#)

62. Crosta, G.B.; Agliardi, F.; Rivolta, C.; Alberti, S.; Dei Cas, L. Long-Term Evolution and Early Warning Strategies for Complex Rockslides by Real-Time Monitoring. *Landslides* **2017**, *14*, 1615–1632. [\[CrossRef\]](#)
63. Béjar-Pizarro, M.; Notti, D.; Mateos, R.M.; Ezquerro, P.; Centolanza, G.; Herrera, G.; Bru, G.; Sanabria, M.; Solari, L.; Duro, J.; et al. Mapping Vulnerable Urban Areas Affected by Slow-Moving Landslides Using Sentinel-1 InSAR Data. *Remote Sens.* **2017**, *9*, 876. [\[CrossRef\]](#)
64. Bardi, F.; Frodella, W.; Ciampalini, A.; Bianchini, S.; Del Ventisette, C.; Gigli, G.; Fanti, R.; Moretti, S.; Basile, G.; Casagli, N. Integration between Ground Based and Satellite SAR Data in Landslide Mapping: The San Fratello Case Study. *Geomorphology* **2014**, *223*, 45–60. [\[CrossRef\]](#)
65. Bianchini, S.; Cigna, F.; Righini, G.; Proietti, C.; Casagli, N. Landslide HotSpot Mapping by Means of Persistent Scatterer Interferometry. *Environ. Earth Sci.* **2012**, *67*, 1155–1172. [\[CrossRef\]](#)
66. Ponziani, F.; Ciuffi, P.; Bayer, B.; Berni, N.; Franceschini, S.; Simoni, A. Regional-Scale InSAR Investigation and Landslide Early Warning Thresholds in Umbria, Italy. *Eng. Geol.* **2023**, *327*, 107352. [\[CrossRef\]](#)
67. Casagli, N.; Catani, F.; Del Ventisette, C.; Luzi, G. Monitoring, Prediction, and Early Warning Using Ground-Based Radar Interferometry. *Landslides* **2010**, *7*, 291–301. [\[CrossRef\]](#)
68. Karunatilake, A.; Zou, L.; Kikuta, K.; Nishimoto, M.; Sato, M. Implementation and Configuration of GB-SAR for Landslide Monitoring: Case Study in Minami-Aso, Kumamoto. *Explor. Geophys.* **2019**, *50*, 210–220. [\[CrossRef\]](#)
69. Bozzano, F.; Mazzanti, P.; Prestininzi, A.; Scarascia Mugnozza, G. Research and Development of Advanced Technologies for Landslide Hazard Analysis in Italy. *Landslides* **2010**, *7*, 381–385. [\[CrossRef\]](#)
70. Del Ventisette, C.; Casagli, N.; Fortuny-Guasch, J.; Tarchi, D. Ruinon Landslide (Valfurva, Italy) Activity in Relation to Rainfall by Means of GBInSAR Monitoring. *Landslides* **2012**, *9*, 497–509. [\[CrossRef\]](#)
71. Lombardi, L.; Nocentini, M.; Frodella, W.; Nolesini, T.; Bardi, F.; Intrieri, E.; Carlà, T.; Solari, L.; Dotta, G.; Ferrigno, F.; et al. The Calatabiano Landslide (Southern Italy): Preliminary GB-InSAR Monitoring Data and Remote 3D Mapping. *Landslides* **2017**, *14*, 685–696. [\[CrossRef\]](#)
72. Guo, Y.; Yang, Y.; Kong, Z.; Gao, C.; Tian, W. Experimental Study on Deformation Monitoring of Large Landslide in Reservoir Area of Hydropower Station Based on GB-InSAR. *Adv. Civ. Eng.* **2021**, *2021*, 5586340. [\[CrossRef\]](#)
73. Intrieri, E.; Gigli, G.; Lombardi, L.; Raspini, F.; Salvatici, T.; Bertolini, G. Integration of Ground-Based Interferometry and Terrestrial Laser Scanning for Rockslide and Rockfall Monitoring. *Rend. Online Della Soc. Geol. Ital.* **2016**, *41*, 243–246. [\[CrossRef\]](#)
74. Ferrigno, F.; Gigli, G.; Fanti, R.; Intrieri, E.; Casagli, N. GB-InSAR Monitoring and Observational Method for Landslide Emergency Management: The Montaguto Earthflow (AV, Italy). *Nat. Hazards Earth Syst. Sci.* **2017**, *17*, 845–860. [\[CrossRef\]](#)
75. De Macedo, K.A.C.; Ramos, F.L.G.; Gaboardi, C.; Moreira, J.R.; Vissirini, F.; Da Costa, M.S. A Compact Ground-Based Interferometric Radar for Landslide Monitoring: The Xerém Experiment. *IEEE J. Sel. Top. Appl. Earth Obs. Remote Sens.* **2017**, *10*, 975–986. [\[CrossRef\]](#)
76. Xiang, X.; Chen, C.; Wang, H.; Lu, H.; Zhang, H.; Chen, J. A Real-Time Processing Method for GB-SAR Monitoring Data by Using the Dynamic Kalman Filter Based on the PS Network. *Landslides* **2023**, *20*, 1639–1655. [\[CrossRef\]](#)
77. Kristensen, L.; Blikra, L.H. Monitoring Displacement on the Mannen Rockslide in Western Norway. In *Landslide Science and Practice*; Margottini, C., Canuti, P., Sassa, K., Eds.; Springer: Berlin/Heidelberg, Germany, 2013; pp. 251–256, ISBN 978-3-642-31444-5. [\[CrossRef\]](#)
78. Atzeni, C.; Barla, M.; Pieraccini, M.; Antolini, F. Early Warning Monitoring of Natural and Engineered Slopes with Ground-Based Synthetic-Aperture Radar. *Rock Mech. Rock Eng.* **2015**, *48*, 235–246. [\[CrossRef\]](#)
79. Puniach, E.; Gruszczyński, W.; Ćwiakała, P.; Matwij, W. Application of UAV-Based Orthomosaics for Determination of Horizontal Displacement Caused by Underground Mining. *ISPRS J. Photogramm. Remote Sens.* **2021**, *174*, 282–303. [\[CrossRef\]](#)
80. Stumpf, A.; Malet, J.-P.; Allemand, P.; Pierrot-Deseilligny, M.; Skupinski, G. Ground-Based Multi-View Photogrammetry for the Monitoring of Landslide Deformation and Erosion. *Geomorphology* **2015**, *231*, 130–145. [\[CrossRef\]](#)
81. Lucieer, A.; Jong, S.M.D.; Turner, D. Mapping Landslide Displacements Using Structure from Motion (SfM) and Image Correlation of Multi-Temporal UAV Photography. *Prog. Phys. Geogr. Earth Environ.* **2014**, *38*, 97–116. [\[CrossRef\]](#)
82. Xu, Q.; Zhao, B.; Dai, K.; Dong, X.; Li, W.; Zhu, X.; Yang, Y.; Xiao, X.; Wang, X.; Huang, J.; et al. Remote Sensing for Landslide Investigations: A Progress Report from China. *Eng. Geol.* **2023**, *321*, 107156. [\[CrossRef\]](#)
83. Lan, H.; Liu, X.; Li, L.; Li, Q.; Tian, N.; Peng, J. Remote Sensing Precursors Analysis for Giant Landslides. *Remote Sens.* **2022**, *14*, 4399. [\[CrossRef\]](#)
84. Wang, H.; Nie, D.; Tuo, X.; Zhong, Y. Research on Crack Monitoring at the Trailing Edge of Landslides Based on Image Processing. *Landslides* **2020**, *17*, 985–1007. [\[CrossRef\]](#)
85. Thapa, P.S.; Adhikari, B.R.; Shaw, R.; Bhattarai, D.; Yanai, S. Geomorphological Analysis and Early Warning Systems for Landslide Risk Mitigation in Nepalese Mid-Hills. *Nat. Hazards* **2023**, *117*, 1793–1812. [\[CrossRef\]](#)
86. Ma, H.-R.; Cheng, X.; Chen, L.; Zhang, H.; Xiong, H. Automatic Identification of Shallow Landslides Based on Worldview2 Remote Sensing Images. *J. Appl. Remote Sens.* **2016**, *10*, 016008. [\[CrossRef\]](#)
87. Guo, Y.; Li, X.; Ju, S.; Lyu, Q.; Liu, T. Utilization of 3D Laser Scanning for Stability Evaluation and Deformation Monitoring of Landslides. *J. Environ. Public Health* **2022**, *2022*, 8225322. [\[CrossRef\]](#)
88. Lohani, B.; Ghosh, S. Airborne LiDAR Technology: A Review of Data Collection and Processing Systems. *Proc. Natl. Acad. Sci. India Sect. A Phys. Sci.* **2017**, *87*, 567–579. [\[CrossRef\]](#)

89. Conte, G.; Kleiner, A.; Rudol, P.; Korwel, K.; Wzorek, M.; Doherty, P. Performance Evaluation of A Light-Weight Multi-Echo Lidar for Unmanned Rotorcraft Applications. *Int. Arch. Photogramm. Remote Sens. Spat. Inf. Sci.* **2013**, *XL-1/W2*, 87–92. [\[CrossRef\]](#)
90. Guerin, A.; Stock, G.M.; Radue, M.J.; Jaboyedoff, M.; Collins, B.D.; Matasci, B.; Avdievitch, N.; Derron, M.-H. Quantifying 40 Years of Rockfall Activity in Yosemite Valley with Historical Structure-from-Motion Photogrammetry and Terrestrial Laser Scanning. *Geomorphology* **2020**, *356*, 107069. [\[CrossRef\]](#)
91. Abellán, A.; Oppikofer, T.; Jaboyedoff, M.; Rosser, N.J.; Lim, M.; Lato, M.J. Terrestrial Laser Scanning of Rock Slope Instabilities. *Earth Surf. Process. Landf.* **2014**, *39*, 80–97. [\[CrossRef\]](#)
92. Blasone, G.; Cavalli, M.; Marchi, L.; Cazorzi, F. Monitoring Sediment Source Areas in a Debris-Flow Catchment Using Terrestrial Laser Scanning. *Catena* **2014**, *123*, 23–36. [\[CrossRef\]](#)
93. Parenti, C.; Rossi, P.; Mancini, F.; Scorpio, V.; Grassi, F.; Ciccacese, G.; Lugli, F.; Soldati, M. Multitemporal Analysis of Slow-Moving Landslides and Channel Dynamics through Integrated Remote Sensing and In Situ Techniques. *Remote Sens.* **2023**, *15*, 3563. [\[CrossRef\]](#)
94. Razak, K.A.; Santangelo, M.; Van Westen, C.J.; Straatsma, M.W.; De Jong, S.M. Generating an Optimal DTM from Airborne Laser Scanning Data for Landslide Mapping in a Tropical Forest Environment. *Geomorphology* **2013**, *190*, 112–125. [\[CrossRef\]](#)
95. Borkowski, A.; Perski, Z.; Wojciechowski, T.; Józków, G.; Wójcik, A. Landslides Mapping in Roznow Lake Vicinity, Poland Using Airborne Laser Scanning Data. *Acta Geodyn. Geomater.* **2011**, *8*, 325–333.
96. Mezaal, M.; Pradhan, B.; Rizeei, H. Improving Landslide Detection from Airborne Laser Scanning Data Using Optimized Dempster–Shafer. *Remote Sens.* **2018**, *10*, 1029. [\[CrossRef\]](#)
97. Ventura, G.; Vilardo, G.; Terranova, C.; Sessa, E.B. Tracking and Evolution of Complex Active Landslides by Multi-Temporal Airborne LiDAR Data: The Montaguto Landslide (Southern Italy). *Remote Sens. Environ.* **2011**, *115*, 3237–3248. [\[CrossRef\]](#)
98. Donati, D.; Stead, D.; Lato, M.; Gaib, S. Spatio-Temporal Characterization of Slope Damage: Insights from the Ten Mile Slide, British Columbia, Canada. *Landslides* **2020**, *17*, 1037–1049. [\[CrossRef\]](#)
99. Travelletti, J.; Delacourt, C.; Malet, J.-P.; Allemand, P.; Schmittbuhl, J.; Toussaint, R. Performance of Image Correlation Techniques for Landslide Displacement Monitoring. In *Landslide Science and Practice*; Margottini, C., Canuti, P., Sassa, K., Eds.; Springer: Berlin/Heidelberg, Germany, 2013; pp. 217–226, ISBN 978-3-642-31444-5.
100. Pfeiffer, J.; Zieher, T.; Bremer, M.; Wichmann, V.; Rutzinger, M. Derivation of Three-Dimensional Displacement Vectors from Multi-Temporal Long-Range Terrestrial Laser Scanning at the Reissenschuh Landslide (Tyrol, Austria). *Remote Sens.* **2018**, *10*, 1688. [\[CrossRef\]](#)
101. Fey, C.; Rutzinger, M.; Wichmann, V.; Prager, C.; Bremer, M.; Zangerl, C. Deriving 3D Displacement Vectors from Multi-Temporal Airborne Laser Scanning Data for Landslide Activity Analyses. *GIScience Remote Sens.* **2015**, *52*, 437–461. [\[CrossRef\]](#)
102. Vollmer, M. Infrared Thermal Imaging. In *Computer Vision*; Ikeuchi, K., Ed.; Springer International Publishing: Cham, Switzerland, 2021; pp. 666–670, ISBN 978-3-030-63415-5.
103. Usamentiaga, R.; Venegas, P.; Guerediaga, J.; Vega, L.; Molleda, J.; Bulnes, F. Infrared Thermography for Temperature Measurement and Non-Destructive Testing. *Sensors* **2014**, *14*, 12305–12348. [\[CrossRef\]](#) [\[PubMed\]](#)
104. Baroň, I.; Bečkovský, D.; Miča, L. Application of Infrared Thermography for Mapping Open Fractures in Deep-Seated Rockslides and Unstable Cliffs. *Landslides* **2014**, *11*, 15–27. [\[CrossRef\]](#)
105. Liao, Z.; Hong, Y.; Wang, J.; Fukuoka, H.; Sassa, K.; Karnawati, D.; Fathani, F. Prototyping an Experimental Early Warning System for Rainfall-Induced Landslides in Indonesia Using Satellite Remote Sensing and Geospatial Datasets. *Landslides* **2010**, *7*, 317–324. [\[CrossRef\]](#)
106. Li, W.; Zhan, W.; Lu, H.; Xu, Q.; Pei, X.; Wang, D.; Huang, R.; Ge, D. Precursors to Large Rockslides Visible on Optical Remote-Sensing Images and Their Implications for Landslide Early Detection. *Landslides* **2023**, *20*, 1–12. [\[CrossRef\]](#)
107. Hungr, O.; Leroueil, S.; Picarelli, L. The Varnes Classification of Landslide Types, an Update. *Landslides* **2014**, *11*, 167–194. [\[CrossRef\]](#)
108. Frodella, W.; Ciampalini, A.; Gigli, G.; Lombardi, L.; Raspini, F.; Nocentini, M.; Scardigli, C.; Casagli, N. Synergic Use of Satellite and Ground Based Remote Sensing Methods for Monitoring the San Leo Rock Cliff (Northern Italy). *Geomorphology* **2016**, *264*, 80–94. [\[CrossRef\]](#)
109. Jacquemart, M.; Tiampo, K. Leveraging Time Series Analysis of Radar Coherence and Normalized Difference Vegetation Index Ratios to Characterize Pre-Failure Activity of the Mud Creek Landslide, California. *Nat. Hazards Earth Syst. Sci.* **2021**, *21*, 629–642. [\[CrossRef\]](#)
110. Tzouvaras, M. Statistical Time-Series Analysis of Interferometric Coherence from Sentinel-1 Sensors for Landslide Detection and Early Warning. *Sensors* **2021**, *21*, 6799. [\[CrossRef\]](#) [\[PubMed\]](#)
111. Liu, B.; He, K.; Han, M.; Hu, X.; Ma, G.; Wu, M. Application of UAV and GB-SAR in Mechanism Research and Monitoring of Zhonghaicun Landslide in Southwest China. *Remote Sens.* **2021**, *13*, 1653. [\[CrossRef\]](#)
112. Deguchi, T.; Sugiyama, T.; Kishimoto, M. Landslide Monitoring by Using Ground-Based Millimeter Wave Radar System. In Proceedings of the 17th European Conference on Soil Mechanics and Geotechnical Engineering (ECSMGE), Reykjavik, Iceland, 1–6 September 2019; International Society for Soil Mechanics and Geotechnical Engineering: London, UK, 2019; pp. 627–632. [\[CrossRef\]](#)
113. Turner, D.; Lucieer, A.; De Jong, S. Time Series Analysis of Landslide Dynamics Using an Unmanned Aerial Vehicle (UAV). *Remote Sens.* **2015**, *7*, 1736–1757. [\[CrossRef\]](#)

114. Pellicani, R.; Argentiero, I.; Manzari, P.; Spilotro, G.; Marzo, C.; Ermini, R.; Apollonio, C. UAV and Airborne LiDAR Data for Interpreting Kinematic Evolution of Landslide Movements: The Case Study of the Montescaglioso Landslide (Southern Italy). *Geosciences* **2019**, *9*, 248. [\[CrossRef\]](#)
115. Huang, R.; Jiang, L.; Shen, X.; Dong, Z.; Zhou, Q.; Yang, B.; Wang, H. An Efficient Method of Monitoring Slow-Moving Landslides with Long-Range Terrestrial Laser Scanning: A Case Study of the Dashu Landslide in the Three Gorges Reservoir Region, China. *Landslides* **2019**, *16*, 839–855. [\[CrossRef\]](#)
116. Kromer, R.; Lato, M.; Hutchinson, D.J.; Gauthier, D.; Edwards, T. Managing Rockfall Risk through Baseline Monitoring of Precursors Using a Terrestrial Laser Scanner. *Can. Geotech. J.* **2017**, *54*, 953–967. [\[CrossRef\]](#)
117. Sun, J.; Yuan, G.; Song, L.; Zhang, H. Unmanned Aerial Vehicles (UAVs) in Landslide Investigation and Monitoring: A Review. *Drones* **2024**, *8*, 30. [\[CrossRef\]](#)
118. Deligiannakis, G.; Pallikarakis, A.; Papanikolaou, I.; Alexiou, S.; Reicherter, K. Detecting and Monitoring Early Post-Fire Sliding Phenomena Using UAV–SfM Photogrammetry and t-LiDAR-Derived Point Clouds. *Fire* **2021**, *4*, 87. [\[CrossRef\]](#)
119. Frodella, W.; Gigli, G.; Morelli, S.; Lombardi, L.; Casagli, N. Landslide Mapping and Characterization through Infrared Thermography (IRT): Suggestions for a Methodological Approach from Some Case Studies. *Remote Sens.* **2017**, *9*, 1281. [\[CrossRef\]](#)
120. Costantini, M.; Minati, F.; Trillo, F.; Ferretti, A.; Novali, F.; Passera, E.; Dehls, J.; Larsen, Y.; Marinkovic, P.; Eineder, M.; et al. European Ground Motion Service (EGMS). In Proceedings of the 2021 IEEE International Geoscience and Remote Sensing Symposium IGARSS, Brussels, Belgium, 11–16 July 2021; IEEE: New York, NY, USA, 2021; pp. 3293–3296. [\[CrossRef\]](#)
121. Bentley, M.J.; Foster, J.M.; Potvin, J.J.; Bevan, G.; Sharp, J.; Woeller, D.J.; Take, W.A. Surface Displacement Expression of Progressive Failure in a Sensitive Clay Landslide Observed with Long-Term UAV Monitoring. *Landslides* **2023**, *20*, 531–546. [\[CrossRef\]](#)
122. Lacroix, P.; Huanca, J.; Albinez, L.; Taipei, E. Precursory Motion and Time-Of-Failure Prediction of the Achoma Landslide, Peru, From High Frequency PlanetScope Satellites. *Geophys. Res. Lett.* **2023**, *50*, e2023GL105413. [\[CrossRef\]](#)
123. Jiao, Q.; Jiang, W.; Qian, H.; Li, Q. Research on Characteristics and Failure Mechanism of Guizhou Shuicheng Landslide Based on InSAR and UAV Data. *Nat. Hazards Res.* **2022**, *2*, 17–24. [\[CrossRef\]](#)
124. Liu, S.; Wang, H.; Huang, J.; Wu, L. High-Resolution Remote Sensing Image-Based Extensive Deformation-Induced Landslide Displacement Field Monitoring Method. *Int. J. Coal Sci. Technol.* **2015**, *2*, 170–177. [\[CrossRef\]](#)
125. Travelletti, J.; Delacourt, C.; Allemand, P.; Malet, J.-P.; Schmittbuhl, J.; Toussaint, R.; Bastard, M. Correlation of Multi-Temporal Ground-Based Optical Images for Landslide Monitoring: Application, Potential and Limitations. *ISPRS J. Photogramm. Remote Sens.* **2012**, *70*, 39–55. [\[CrossRef\]](#)
126. Yang, W.; Liu, L.; Shi, P. Detecting Precursors of an Imminent Landslide along the Jinsha River. *Nat. Hazards Earth Syst. Sci.* **2020**, *20*, 3215–3224. [\[CrossRef\]](#)
127. Qi, W.; Yang, W.; He, X.; Xu, C. Detecting Chamoli Landslide Precursors in the Southern Himalayas Using Remote Sensing Data. *Landslides* **2021**, *18*, 3449–3456. [\[CrossRef\]](#)
128. Khan, M.W.; Dunning, S.; Bainbridge, R.; Martin, J.; Diaz-Moreno, A.; Torun, H.; Jin, N.; Woodward, J.; Lim, M. Low-Cost Automatic Slope Monitoring Using Vector Tracking Analyses on Live-Streamed Time-Lapse Imagery. *Remote Sens.* **2021**, *13*, 893. [\[CrossRef\]](#)
129. Bernardo, E.; Barrile, V.; Fotia, A. Innovative UAV Methods for Intelligent Landslide Monitoring. In Proceedings of the International Conference of Young Professionals «GeoTerrace-2020», Lviv, Ukraine, 7–9 December 2020; European Association of Geoscientists & Engineers: Bunnik, The Netherlands, 2020; pp. 1–5.
130. Bernardo, E.; Palamara, R.; Boima, R. UAV and Soft Computing Methodology for Monitoring Landslide Areas (Susceptibility to Landslides and Early Warning). *WSEAS Trans. Environ. Dev.* **2021**, *17*, 490–501. [\[CrossRef\]](#)
131. Xie, M.; Zhao, W.; Ju, N.; He, C.; Huang, H.; Cui, Q. Landslide Evolution Assessment Based on InSAR and Real-Time Monitoring of a Large Reactivated Landslide, Wenchuan, China. *Eng. Geol.* **2020**, *277*, 105781. [\[CrossRef\]](#)
132. Kristensen, L.; Czekirda, J.; Penna, I.; Etzelmüller, B.; Nicolet, P.; Pullarello, J.S.; Blikra, L.H.; Skrede, I.; Oldani, S.; Abellan, A. Movements, Failure and Climatic Control of the Veslemannen Rockslide, Western Norway. *Landslides* **2021**, *18*, 1963–1980. [\[CrossRef\]](#)
133. Fan, X.; Xu, Q.; Alonso-Rodriguez, A.; Subramanian, S.S.; Li, W.; Zheng, G.; Dong, X.; Huang, R. Successive Landsliding and Damming of the Jinsha River in Eastern Tibet, China: Prime Investigation, Early Warning, and Emergency Response. *Landslides* **2019**, *16*, 1003–1020. [\[CrossRef\]](#)
134. Guilhot, D.; Martinez Del Hoyo, T.; Bartoli, A.; Ramakrishnan, P.; Leemans, G.; Houtepen, M.; Salzer, J.; Metzger, J.S.; Maknavicius, G. Internet-of-Things-Based Geotechnical Monitoring Boosted by Satellite InSAR Data. *Remote Sens.* **2021**, *13*, 2757. [\[CrossRef\]](#)
135. Bian, S.; Chen, G.; Zeng, R.; Meng, X.; Jin, J.; Lin, L.; Zhang, Y.; Shi, W. Post-Failure Evolution Analysis of an Irrigation-Induced Loess Landslide Using Multiple Remote Sensing Approaches Integrated with Time-Lapse ERT Imaging: Lessons from Heifangtai, China. *Landslides* **2022**, *19*, 1179–1197. [\[CrossRef\]](#)
136. Svennevig, K.; Dahl-Jensen, T.; Keiding, M.; Merryman Boncori, J.P.; Larsen, T.B.; Salehi, S.; Munck Solgaard, A.; Voss, P.H. Evolution of Events before and after the 17 June 2017 Rock Avalanche at Karrat Fjord, West Greenland—A Multidisciplinary Approach to Detecting and Locating Unstable Rock Slopes in a Remote Arctic Area. *Earth Surf. Dyn.* **2020**, *8*, 1021–1038. [\[CrossRef\]](#)
137. Demurtas, V.; Emanuele Orru, P.; Deiana, G. Active Lateral Spreads Monitoring System in East-Central Sardinia. *Eur. J. Remote Sens.* **2022**, *56*, 2161418. [\[CrossRef\]](#)

138. Keuschnig, M.; Schober, A.; Delleske, R.; Brandner, K.; Höfer-Öllinger, G. Scale-Oriented Landslide Monitoring and Early Warning System for Uranium Legacy Complexes in Mailuu Suu, Kyrgyzstan. *Geomech. Tunn.* **2021**, *14*, 47–53. [\[CrossRef\]](#)
139. Ciampalini, A.; Farina, P.; Lombardi, L.; Nocentini, M.; Taurino, V.; Guidi, R.; Pina, F.D.; Tavarini, D. Integration of Satellite InSAR with a Wireless Network of Geotechnical Sensors for Slope Monitoring in Urban Areas: The Pariana Landslide Case (Massa, Italy). *Remote Sens.* **2021**, *13*, 2534. [\[CrossRef\]](#)
140. Xiao, T.; Huang, W.; Deng, Y.; Tian, W.; Sha, Y. Long-Term and Emergency Monitoring of Zhongbao Landslide Using Space-Borne and Ground-Based InSAR. *Remote Sens.* **2021**, *13*, 1578. [\[CrossRef\]](#)
141. Meng, Q.; Xu, Q.; Wang, B.; Li, W.; Peng, Y.; Peng, D.; Qi, X.; Zhou, D. Monitoring the Regional Deformation of Loess Landslides on the Heifangtai Terrace Using the Sentinel-1 Time Series Interferometry Technique. *Nat. Hazards* **2019**, *98*, 485–505. [\[CrossRef\]](#)
142. Catani, F.; Canuti, P.; Casagli, N. The Use of Radar Interferometry in Landslide Monitoring. In *Landslides in Cold Regions in the Context of Climate Change*; Shan, W., Guo, Y., Wang, F., Marui, H., Strom, A., Eds.; Environmental Science and Engineering; Springer International Publishing: Cham, Switzerland, 2014; pp. 177–190, ISBN 978-3-319-00866-0.
143. Zheng, X.; Yang, X.; Ma, H.; Ren, G.; Yu, Z.; Yang, F.; Zhang, H.; Gao, W. Integrative Landslide Emergency Monitoring Scheme Based on GB-INSAR Interferometry, Terrestrial Laser Scanning and UAV Photography. *J. Phys. Conf. Ser.* **2019**, *1213*, 052069. [\[CrossRef\]](#)
144. Hermle, D.; Keuschnig, M.; Hartmeyer, I.; Delleske, R.; Krautblatter, M. Timely Prediction Potential of Landslide Early Warning Systems with Multispectral Remote Sensing: A Conceptual Approach Tested in the Sattelkar, Austria. *Nat. Hazards Earth Syst. Sci.* **2021**, *21*, 2753–2772. [\[CrossRef\]](#)
145. Thirugnanam, H.; Uhlemann, S.; Reghunadh, R.; Ramesh, M.V.; Rangan, V.P. Review of Landslide Monitoring Techniques With IoT Integration Opportunities. *IEEE J. Sel. Top. Appl. Earth Obs. Remote Sens.* **2022**, *15*, 5317–5338. [\[CrossRef\]](#)
146. Manconi, A. How Phase Aliasing Limits Systematic Space-Borne DInSAR Monitoring and Failure Forecast of Alpine Landslides. *Eng. Geol.* **2021**, *287*, 106094. [\[CrossRef\]](#)
147. Chae, B.-G.; Park, H.-J.; Catani, F.; Simoni, A.; Berti, M. Landslide Prediction, Monitoring and Early Warning: A Concise Review of State-of-the-Art. *Geosci. J.* **2017**, *21*, 1033–1070. [\[CrossRef\]](#)
148. Xiang, X.; Chen, C.; Wang, H.; Xing, C.; Chen, J.; Zhu, H. An Improved Method of GB-SAR Phase Unwrapping for Landslide Monitoring. *Front. Earth Sci.* **2022**, *10*, 973320. [\[CrossRef\]](#)
149. Ma, D.; Li, Y.; Cai, J.; Li, B.; Liu, Y.; Chen, X. Real-Time Diagnosis of Island Landslides Based on GB-RAR. *J. Mar. Sci. Eng.* **2020**, *8*, 192. [\[CrossRef\]](#)
150. Cosentino, A.; Marmoni, G.M.; Fiorucci, M.; Mazzanti, P.; Scarascia Mugnozza, G.; Esposito, C. Optical and Thermal Image Processing for Monitoring Rainfall Triggered Shallow Landslides: Insights from Analogue Laboratory Experiments. *Remote Sens.* **2023**, *15*, 5577. [\[CrossRef\]](#)
151. Li, M.; Zhang, L.; Ding, C.; Li, W.; Luo, H.; Liao, M.; Xu, Q. Retrieval of Historical Surface Displacements of the Baige Landslide from Time-Series SAR Observations for Retrospective Analysis of the Collapse Event. *Remote Sens. Environ.* **2020**, *240*, 111695. [\[CrossRef\]](#)
152. Moretto, S.; Bozzano, F.; Esposito, C.; Mazzanti, P.; Rocca, A. Assessment of Landslide Pre-Failure Monitoring and Forecasting Using Satellite SAR Interferometry. *Geosciences* **2017**, *7*, 36. [\[CrossRef\]](#)
153. Schwarz, K.; Heitkötter, J.; Heil, J.; Marschner, B.; Stumpe, B. The Potential of Active and Passive Infrared Thermography for Identifying Dynamics of Soil Moisture and Microbial Activity at High Spatial and Temporal Resolution. *Geoderma* **2018**, *327*, 119–129. [\[CrossRef\]](#)
154. Mengen, D.; Montzka, C.; Jagdhuber, T.; Fluhrer, A.; Brogi, C.; Baum, S.; Schüttemeyer, D.; Bayat, B.; Bogen, H.; Coccia, A.; et al. The Sarsense Campaign: Air- and Space-Borne C- and L-Band SAR for the Analysis of Soil and Plant Parameters in Agriculture. *Remote Sens.* **2021**, *13*, 825. [\[CrossRef\]](#)
155. Tomás, R.; Zeng, Q.; Lopez-Sanchez, J.M.; Zhao, C.; Li, Z.; Liu, X.; Navarro-Hernández, M.I.; Hu, L.; Luo, J.; Díaz, E.; et al. Advances on the Investigation of Landslides by Space-Borne Synthetic Aperture Radar Interferometry. *Geo-Spat. Inf. Sci.* **2023**, *27*, 602–623. [\[CrossRef\]](#)
156. Shi, X.; Zhang, L.; Liao, M.; Balz, T. Landslide Monitoring in Three Gorges Area by Joint Use of Phase Based and Amplitude Based Methods. In Proceedings of the Proceedings of Fringe 2015: Advances in the Science and Applications of SAR Interferometry and Sentinel-1 InSAR Workshop, Frascati, Italy, 23–27 March 2015; European Space Agency: Paris, France, 2015.
157. Deguchi, T.; Sugiyama, T.; Kishimoto, M. On the Development of Ground-Based and Drone-Borne Radar System. In *Recent Research on Engineering Geology and Geological Engineering, Proceedings of the 2nd GeoMEast International Congress and Exhibition on Sustainable Civil Infrastructures, Egypt 2018—The Official International Congress of the Soil-Structure Interaction Group in Egypt (SSIGE), Cairo, Egypt, 24–28 November 2018*; Wasowski, J., Dijkstra, T., Eds.; Springer International Publishing: Cham, Switzerland, 2019; ISBN 978-3-030-02031-6.
158. Zheng, X.; He, G.; Wang, S.; Wang, Y.; Wang, G.; Yang, Z.; Yu, J.; Wang, N. Comparison of Machine Learning Methods for Potential Active Landslide Hazards Identification with Multi-Source Data. *ISPRS Int. J. Geo-Inf.* **2021**, *10*, 253. [\[CrossRef\]](#)
159. Zhang, T.; Zhang, W.; Cao, D.; Yi, Y.; Wu, X. A New Deep Learning Neural Network Model for the Identification of InSAR Anomalous Deformation Areas. *Remote Sens.* **2022**, *14*, 2690. [\[CrossRef\]](#)

160. Nava, L.; Carraro, E.; Reyes-Carmona, C.; Puliero, S.; Bhuyan, K.; Rosi, A.; Monserrat, O.; Floris, M.; Meena, S.R.; Galve, J.P.; et al. Landslide Displacement Forecasting Using Deep Learning and Monitoring Data across Selected Sites. *Landslides* **2023**, *20*, 2111–2129. [[CrossRef](#)]
161. Thiebes, B.; Glade, T. Landslide Early Warning Systems—Fundamental Concepts and Innovative Applications. In *Landslides and Engineered Slopes. Experience, Theory and Practice, Proceedings of the 12th International Symposium on Landslides, Naples, Italy, 12–19 June 2016*; CRC Press: Boca Raton, FL, USA, 2016; pp. 1903–1911.
162. Catani, F. Landslide Detection by Deep Learning of Non-Nadir and Crowdsourced Optical Images. *Landslides* **2021**, *18*, 1025–1044. [[CrossRef](#)]
163. Vassileva, M.; Motagh, M.; Roessner, S.; Xia, Z. Reactivation of an Old Landslide in North–Central Iran Following Reservoir Impoundment: Results from Multisensor Satellite Time-Series Analysis. *Eng. Geol.* **2023**, *327*, 107337. [[CrossRef](#)]
164. Hussain, Y.; Schlögel, R.; Innocenti, A.; Hamza, O.; Iannucci, R.; Martino, S.; Havenith, H.-B. Review on the Geophysical and UAV-Based Methods Applied to Landslides. *Remote Sens.* **2022**, *14*, 4564. [[CrossRef](#)]
165. Fang, K.; Dong, A.; Tang, H.; An, P.; Wang, Q.; Jia, S.; Zhang, B. Development of an Easy-Assembly and Low-Cost Multismartphone Photogrammetric Monitoring System for Rock Slope Hazards. *Int. J. Rock Mech. Min. Sci.* **2024**, *174*, 105655. [[CrossRef](#)]

Disclaimer/Publisher’s Note: The statements, opinions and data contained in all publications are solely those of the individual author(s) and contributor(s) and not of MDPI and/or the editor(s). MDPI and/or the editor(s) disclaim responsibility for any injury to people or property resulting from any ideas, methods, instructions or products referred to in the content.